Controlling Semiconductor/Metal Junction Barriers by Incomplete, Nonideal Molecular Monolayers

ARTICLE *in* JOURNAL OF THE AMERICAN CHEMICAL SOCIETY · JUNE 2006

Impact Factor: 12.11 · DOI: 10.1021/ja058224a · Source: PubMed

J|A|C|S
ARTICLES
Published on Web 05/06/2006

Controlling Semiconductor/Metal Junction Barriers by Incomplete, Nonideal Molecular Monolayers

Hossam Haick,[†,⊥] Marianna Ambrico,[‡] Teresa Ligonzo,[§] Raymond T. Tung,[||] and David Cahen*[,⊥]

Contribution from the Department of Materials and Interfaces, Weizmann Institute of Science, Rehovot 76100, Israel, CNR-IMIP, Sezione di Bari, Via Orabona, 4 I-70126 Bari, Italy, Dipartimento di Fisica Universita' degli Studi di Bari and INFM, Via Orabona, 4 I-70126 Bari, Italy, and Department of Physics, Brooklyn College, City University of New York, Brooklyn, New York 11210

Received December 3, 2005; E-mail: david.cahen@weizmann.ac.il

Abstract: We study how partial monolayers of molecular dipoles at semiconductor/metal interfaces can affect electrical transport across these interfaces, using a series of molecules with systematically varying dipole moment, adsorbed on *n*-GaAs, prior to Au or Pd metal contact deposition, by indirect evaporation or as "ready-made" pads. From analyses of the molecularly modified surfaces, we find that molecular coverage is poorer on low- than on high-doped *n*-GaAs. Electrical charge transport across the resulting interfaces was studied by current−voltage−temperature, internal photoemission, and capacitance−voltage measurements. The data were analyzed and compared with numerical simulations of interfaces that present inhomogeneous barriers for electron transport across them. For high-doped GaAs, we confirm that only the former, molecular dipole-dependent barrier is found. Although no clear molecular effects appear to exist with low-doped *n*-GaAs, those data are well explained by two coexisting barriers for electron transport, one with clear systematic dependence on molecular dipole (molecule-controlled regions) and a constant one (molecule-free regions, pinholes). This explains why directly observable molecular control over the barrier height is found with high-doped GaAs: there, the monolayer pinholes are small enough for their electronic effect not to be felt (they are "pinched off"). We conclude that molecules can control and tailor electronic devices need not form high-quality monolayers, bind chemically to both electrodes, or form multilayers to achieve complete surface coverage. Furthermore, the problem of stability during electron transport is significantly alleviated with molecular control via partial molecule coverage, as most current flows now between, rather than via, the molecules.

1. Introduction

Control over the electronic properties of semiconductors and metals is a central issue for their use in (opto)electronic devices. Modifying a solid's properties by changing its composition (e.g., via doping) is possible only within certain, generally narrow limits due to thermodynamic constraints.[1,2] Designing systems with interfaces, whose electrical properties can be varied, provides a significant degree of control over the system's electrical characteristics because electronic transport through devices depends critically on the properties of the interfaces through which electrons pass.[3−6]

The use of molecules to modify and tailor *material* properties is attractive in (opto)electronic *devices* because of the molecules' functional variety and flexibility.[7−11] In hybrid devices, molecular functionality serves to influence and control characteristics of "classical" electronic devices. This approach to molecular electronics has the potential advantage over others in its links with existing know-how, providing high "added value". Earlier results have shown that molecular layers can modify the *surface* properties of semiconductors significantly.[9,12−16] Examples

† Chemical Engineering, Technion, Haifa 32000, Israel.
‡ Sezione di Bari.
§ Universita' degli Studi di Bari and INFM.
|| City University of New York.
⊥ Weizmann Institute of Science.

(1) Gersten, J. I.; Smith, F. W. *The Physics and Chemistry of Materials*; Wiley: New York, 2001.
(2) Cahen, D.; Chernyak, L. *Adv. Mater.* **1997**, *9*, 861−876.
(3) Hsu, J. W. P. *Mater. Today* **2005**, *8*, 42−54.
(4) Hipps, K. W. *Science* **2001**, *294*, 536−537.
(5) Kushmerick, J. G. *Mater. Today* **2005**, *8*, 26−30.
(6) Cahen, D.; Kahn, A.; Umbach, E. *Mater. Today* **2005**, *8*, 32−41.
(7) Rampi, M. A.; Whitesides, G. M. *Chem. Phys.* **2002**, *281*, 373−391.
(8) Salomon, A.; Cahen, D.; Lindsay, S.; Tomfohr, J.; Engelkes, V. B.; Frisbie, C. D. *Adv. Mater.* **2004**, *16*, 477.
(9) Cahen, D.; Hodes, G. *Adv. Mater.* **2002**, *14*, 789−798.
(10) Shen, Y.; Hosseini, A. R.; Wong, M. H.; Malliaras, G. G. *ChemPhysChem* **2004**, *5*, 16−25.
(11) Chabinyc, M. L.; Chen, X.; Holmlin, R. E.; Jacobs, H.; Skulason, H.; Frisbie, C. D.; Mujica, V.; Ratner, M. A.; Rampi, M. A.; Whitesides, G. M. *J. Am. Chem. Soc.* **2002**, *124*, 11730−11736.
(12) Hsu, J. W. P.; Loo, Y. L.; Lang, D. V.; Rogers, J. A. *J. Vac. Sci. Technol., B* **2003**, *21*, 1928−1935.
(13) Lebedev, M. V. *Prog. Surf. Sci.* **2002**, *70*, 153−186.
(14) Ashkenasy, G.; Cahen, D.; Cohen, R.; Shanzer, A.; Vilan, A. *Acc. Chem. Res.* **2002**, *35*, 121−128.
(15) Seker, F.; Meeker, K.; Kuech, T. F.; Ellis, A. B. *Chem. Rev.* **2000**, *100*, 2505−2536.
(16) Lodha, S.; Janes, D. B. *Appl. Phys. Lett.* **2004**, *85*, 2809−2811.

10.1021/ja058224a CCC: $33.50

include physical protection,[17] optical activity via molecule excitation,[18] and selective electrical[19] and magnetic sensitivity[20] via molecules.

A layer of electrical dipoles on a surface, with a net layer dipole moment perpendicular to the substrate, can produce a substantial shift in surface potentials, i.e., in the work function, φ_m,[21−23] of a metal and in the electron affinity, χ_{sc}, and work function, φ_{sc},[14,24,25] of a semiconductor. To a first-order approximation, the shift arises from how the distribution of the dipoles at the interface perturbs the potential of the electrons in the bulk phase. Although the dipole effect is a general one, use of *molecules* as dipoles allows systematic tuning of the dipole moment, beyond what is obtainable by varying surface-dipole density.

Earlier, we showed that the electron affinity of several semiconductors (CdTe, CdSe, GaAs, polycrystalline $CuInSe_2$, and CdTe) can be changed systematically by adsorbing sets of benzoic and dicarboxylic acid molecules, with varying dipole moments (by changing a given substituent in the molecules) but identical binding to the semiconductor substrates.[14,26] Adding a monolayer of molecules with a positive dipole increased the semiconductor electron affinity, whereas use of a negative molecular dipole decreased it.[27] Similar electron affinity modifications were observed for TiO_2,[28] In:SnO_2 (ITO),[29,30] and ZnO.[31] These effects are remarkable as none of the molecules used in these studies (cf. also Figure 1b) were close-packing ones. Indeed, surface coverage was estimated to be significantly less than full, from 50% up.

Transferring the molecular dipole layer effect from surfaces to interfaces requires making electrical contact to the molecules.[9] This is not at all trivial because normal contacting methods will damage molecules,[32] even if at times such damage is controllable (e.g., by use of a sacrificial end group on molecules[33−35]), and cause shorts because of metal penetration in pinholes or even between molecules.[32,36] Still, using soft contacting methods on

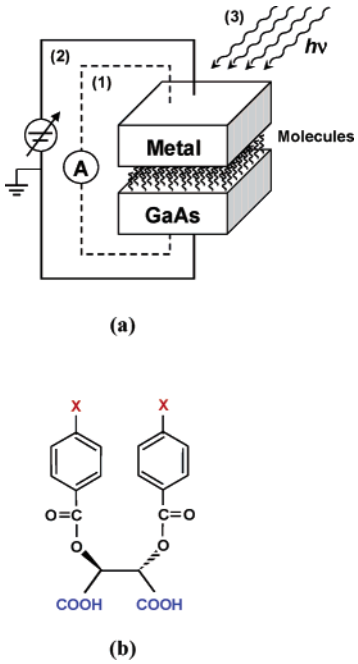

Figure 1. (a) Scheme of the experimental setup used to probe Au/molecules/GaAs junctions by: (1) *I*−*V*, (2) *C*−*V*, and (3) IPE measurements. (b) Chemical formula of the dicarboxylic acids (dC−X) used to modify Au/*n*-GaAs junctions. Changing the substituent ("X" in the formula) changes the free dipole moment of the molecules.

n- and *p*-GaAs and ZnO, the incomplete molecular dipole monolayers, used earlier for surface-potential modification, were found to yield changes in the electrical characteristics of the metal contact/molecularly modified semiconductor junctions that correlated with the free molecule's dipole.[37] Furthermore, varying a soft contacting method (LOFO; cf. ref 38) showed that intimate contact between the molecules' exposed substituents (cf. Figure 1b) and the (top) metal contact completely inverts the molecular dipole effect on the electrical characteristics of the resulting GaAs devices.[39] This behavior was explained by effective dipole inversion due to metal−molecule polarization and partial charge redistribution between metal and molecules[39] (cf. also refs 40 and 41).

A similar effect, suggesting dipole inversion, was found if Au contacts were evaporated (*indirectly*, on a cooled substrate) on the molecules on *n*-GaAs.[36,42] If Pd, instead of Au, was used, no such inversion was observed.[32,36] This striking difference could be attributed to the difference in growth mechanisms of the Pd and Au films, viz., two-dimensional (2D) and three-dimensional (3D) growth, respectively, that leads to differences in the metal's interaction with the molecules.[42] All these effects and others (cf. for example ref 43) stress the importance for electron transport measurements of the nature of the electrical contact to a molecule and of possible metal penetration between molecules.[36]

(17) Ulman, A. *Chem. Rev.* **1996**, *96*, 1533−1554.
(18) Hagfeldt, A.; Graetzel, M. *Acc. Chem. Res.* **2000**, *33*, 269−277.
(19) Heath, J. R.; Ratner, M. A. *Phys. Today* **2003**, *56*, 43−49.
(20) Carmeli, I.; Skakalova, V.; Naaman, R.; Vager, Z. *Angew. Chem., Int. Ed.* **2002**, *41*, 761−764.
(21) Campbell, I. H.; Rubin, S.; Zawodzinski, T. A.; Kress, J. D.; Martin, R. L.; Smith, D. L.; Barashkov, N. N.; Ferrariis, J. P. *Phys. Rev. B: Condens. Matter Mater. Phys.* **1996**, *54*, R14321−R14324.
(22) Evans, S. D.; Ulman, A. *Chem. Phys. Lett.* **1990**, *170*, 462−6.
(23) Bruening, M.; Cohen, R.; Guillemoles, J. F.; Moav, T.; Libman, J.; Shanzer, A.; Cahen, D. *J. Am. Chem. Soc.* **1997**, *119*, 5720−5728.
(24) Taylor, D. M.; Bayes, G. F. *Phys. Rev. E: Stat. Phys., Plasmas, Fluids, Relat. Interdiscip. Top.* **1994**, *49*, 1439−1449.
(25) Iozzi, M. F.; Cossi, M. *J. Phys. Chem. B* **2005**, *109*, 15383−15390.
(26) Vilan, A.; Cahen, D. *Trends Biotechnol.* **2002**, *20*, 22−29.
(27) The dipole moment is a vector, oriented from the (−) to the (+) charge. We define as negative a dipole whose negative pole is closer to the semiconductor surface than its positive one. Because of its parallel orientation with the electric field at the surface of an *n*-type semiconductor, a negative dipole is more stable than a positive dipole because of the antiparallel alignment with respect to the field.
(28) Kruger, J.; Bach, U.; Gratzel, M. *Adv. Mater.* **2000**, *12*, 447−451.
(29) Nuesch, F.; Rotzinger, F.; Si-Ahmed, L.; Zuppiroli, L. *Chem. Phys. Lett.* **1998**, *288*, 861−867.
(30) Ganzorig, C.; Kwak, K.-J.; Yagi, K.; Fujihira, M. *Appl. Phys. Lett.* **2001**, *79*, 272−274.
(31) Salomon, A.; Berkovich, D.; Cahen, D. *Appl. Phys. Lett.* **2003**, *82*, 1051−1053.
(32) Haick, H.; Ambrico, M.; Ghabboun, J.; Ligonzo, T.; Cahen, D. *Phys. Chem. Chem. Phys.* **2004**, *6*, 4538−4541.
(33) Fisher, G. L.; Hooper, A. E.; Opila, R. L.; Allara, D. L.; Winograd, N. *J. Phys. Chem. B* **2000**, *104*, 3267−3273.
(34) Fisher, G. L.; Walker, A. V.; Hooper, A. E.; Tighe, T. B.; Bahnck, K. B.; Skriba, H. T.; Reinard, M. D.; Haynie, B. C.; Opila, R. L.; Winograd, N.; Allara, D. L. *J. Am. Chem. Soc.* **2002**, *124*, 5528−5541.
(35) Jung, D. R.; Czanderna, A. W.; Herdt, G. C. *J. Vac. Sci. Technol., A* **1996**, *14*, 1779−1787.
(36) Haick, H.; Ghabboun, J.; Cahen, D. *Appl. Phys. Lett.* **2005**, *86*, 042113/1−042113/3.
(37) Vilan, A.; Shanzer, A.; Cahen, D. *Nature* **2000**, *404*, 166−168.
(38) Vilan, A.; Cahen, D. *Adv. Funct. Mater.* **2002**, *12*, 795−807.
(39) Vilan, A.; Ghabboun, J.; Cahen, D. *J. Phys. Chem. B* **2003**, *107*, 6360−6376.
(40) Ishii, H.; Sugiyama, H.; Ito, E.; Seki, K. *Adv. Mater.* **1999**, *11*, 605−625.
(41) Crispin, X.; Geskin, V.; Crispin, A.; Cornil, J.; Lazzaroni, R.; Salaneck, W. R.; Bredas, J. L. *J. Am. Chem. Soc.* **2002**, *124*, 8131−8141.
(42) Haick, H.; Ghabboun, J.; Niitsoo, O.; Cohen, H.; Cahen, D.; Vilan, A.; Hwang, J.; Wan, A.; Amy, F.; Kahn, A. *J. Phys. Chem. B* **2005**, *109*, 9622−9630.
(43) Carrara, M.; Nuesch, F.; Zuppiroli, L. *Synth. Met.* **2001**, *121*, 1633−1634.

Remarkably, in all these cases we found systematic variations of the electron transport characteristics with the molecular dipoles, even though the molecules are neither well organized nor close-packed but, rather, form monolayers with a significant fraction of pinholes. To understand how this is possible, we looked for a system with, on one hand, a higher density of or larger area pinholes than what we had studied hitherto and, on the other hand, as similar as possible to the one studied before. As will be shown, using low-doped GaAs, rather than the relatively high-doped samples that we used until now, achieves exactly this.

We conclude that the best description for our experimental results on charge transport across metal/molecules/low-doped GaAs interfaces is in terms of a model of parallel conductance through a discontinuous interface, i.e., the presence of more than one barrier height at the interface. To reach this conclusion, we performed complementary electrical characterizations (cf. Figure 1a) of Au/ and Pd/molecular monolayer/*n*-GaAs junctions, using a series of molecules with systematically varying dipole moments (Figure 1b) as one of our experimental tools, as these molecules were already shown to yield systematic changes in χ_{sc} of n^+- and p^+-GaAs.[39] We then analyzed the data, taking into account the basic assumptions and limitations inherent in each of the measurement techniques[12,44−46] (cf. Supporting Information, section 1).

Our analysis implies an *inhomogeneous* interface, where tunneling *through* the molecules is negligible compared to transport via the pinholes. This finding implies that essentially all the current flows through the pinholes but that with low-doped *n*-GaAs there are two types of these, one with a barrier for transport that is not influenced by the molecules (which is absent with high-doped *n*-GaAs) and another type with a molecule-controlled barrier. This behavior is possible because the molecules exert electrostatic control inside the semiconductor over charge transport through the smaller pinholes. Such electrostatic control then explains the earlier results on high-doped *n*-GaAs, *p*-GaAs,[39] and ZnO[31] with these and related types of molecules, which cannot form completely covering monolayers, because on those surfaces, apparently only small pinholes exist. The implications of this conclusion for the chemistry of molecule-based electronics[47] led us to study such molecular monolayers and their electrical effects as well as possible, so as to check and test the above-mentioned model. Although several spectroscopic techniques gave indications about the apparent quality of the adsorbed monolayers,[23,48] those and other common techniques for monolayer characterization were insufficient to test the model experimentally. We note that high-resolution scanning probe microscopy (SPM) cannot provide the desired information, because the vertical dimensions of many molecules, including the ones used here, are less than or comparable to the surface roughness of the semiconductor substrate. In atomic force microscopy (AFM)-based methods, the tip also tends to move the molecules, making detection of pinholes notoriously difficult.[49,50] A preliminary report on our study can be found in ref 51.

2. Experimental Section

n-GaAs wafers (100), Si doped to $3-4 \times 10^{18}$ cm^{-3} (high-doped, n^+-GaAs) or 2×10^{16} cm^{-3} (low-doped, n^--GaAs) were used. $E_c - E_f$ at room temperature is −0.02 and 0.08 eV for n^+-GaAs and n^--GaAs, respectively.

2.1. Sample Preparation. GaAs substrates were cleaned by sequential immersion for 10 min in hot chloroform, acetone, and in methanol, followed by ozone oxidation for 10 min (in a UVOCs apparatus). The oxide was removed by a 50 s dip in a NH_4OH/H_2O (1:10 v/v) solution, after which the samples were immersed for 5 s in 18 MΩ deionized water followed by acetonitrile (ACN) and then immediately placed in the adsorption solution.

GaAs surfaces that had been cleaned in this way were modified by overnight adsorption from 2.5 mM solution in ACN with dicarboxylic acids (dC−X),[38,52] where "X" (= OCH_3, CH_3, H, CN, and CF_3) stands for the group opposite the binding group (cf. Figure 1b), the terminal group. This group is the one that determines the dipole of the free molecule and is the one that is directly exposed to the outside, i.e., also to the metal that is deposited on the molecules. Earlier we showed that the carboxylic acid binds to GaAs via the Ga sites, rather than the As ones, yielding a carboxylate bridge between Ga atoms.[42,48,53,54] The double-binding group increases the adsorption constant.[54] The presence of the molecules on the surface was verified by contact angle measurements and ellipsometry,[38,55] which showed film thickness of ∼1 nm. Chemical adsorption was verified by Fourier transform infrared (FTIR) spectroscopy, time-of-flight secondary ion mass spectroscopy (TOF SIMS), and, for X = CF_3, by X-ray photoelectron spectroscopy.[42] In addition, molecular film-induced changes in the electrical surface potential were measured as contact potential difference (CPD) by a Kelvin probe.[39,48] Molecules were synthesized as described elsewhere.[48]

2.2. Contact Angle. Advancing sessile drop contact angle of water to contact-free, bare and molecularly modified surfaces was measured by a Ramé-Hart automated contact angle goniometer. Angles were extracted by RHI 2001 imaging software at both sides of the drop, 5 times, at a rate of 1 reading per second.

2.3. Fourier Transform Infrared (FTIR) Spectroscopy. FTIR measurements were performed in the transmission mode using a Bruker Equinox 55 instrument in a N_2-purged chamber to check the adsorption of dC−X ligands on GaAs. Here, IR radiation passes through the (relatively) transparent (300 μm) n^+-GaAs or n^--GaAs wafer, and absorption of the monolayer is recorded using a Mercury Cadmium Telluride (MCT) detector for optimal sensitivity to infrared radiance from 400 to 2000 cm^{-1}. To verify chemical binding, the spectral regions where the O−C−O groups of the carboxylic acid and carboxylate absorb (∼1650 cm^{-1})[53] were used. KBr pellets with similar molar concentrations of dC−X derivatives showed similar absorption intensities, which indicates that the IR extinction coefficients for all dC−X molecules are similar. To compare the adsorption of dC−X ligands on GaAs, we subtracted the IR spectrum of the bare n^+-GaAs or n^--GaAs from the IR spectrum of the molecularly modified n^+-GaAs or n^--GaAs, respectively. The spectral region where the O−C−O groups adsorb is presented in Table 1, after such subtractions.

(44) Loo, Y.-L.; Lang, D. V.; Rogers, J. A.; Hsu, J. W. P. *Nano Lett.* **2003**, *3*, 913.
(45) Schroder, D. K. *Semiconductor Material and Device Characterization*; Wiley: New York, 1990.
(46) Tung, R. T. *Mater. Sci. Eng., R* **2001**, *R35*, 1−138.
(47) Cahen, D.; Naaman, R.; Vager, Z. *Adv. Funct. Mater.* **2005**, *15*, 1571−1578.
(48) Cohen, R.; Kronik, L.; Shanzer, A.; Cahen, D.; Liu, A.; Rosenwaks, Y.; Lorenz, J. K.; Ellis, A. B. *J. Am. Chem. Soc.* **1999**, *121*, 10545−10553.
(49) Liu, G.-Y.; Xu, S.; Qian, Y. *Acc. Chem. Res.* **2000**, *33*, 457−466.
(50) Cohen, S. R. *Scanning Probe Microscopy: Electrical and Electromechanical Characteri-zation at the Nanoscale*; Springer-Verlag, in press.
(51) Haick, H.; Ambrico, M.; Ligonzo, T.; Cahen, D. *Adv. Mater.* **2004**, *16*, 2145−2151.
(52) Cohen, R.; Bastide, S.; Cahen, D.; Libman, J.; Shanzer, A.; Rosenwaks, Y. *Opt. Mater.* **1998**, *9*, 394−400.
(53) Bastide, S.; Butruille, R.; Cahen, D.; Dutta, A.; Libman, J.; Shanzer, A.; Sun, L.; Vilan, A. *J. Phys. Chem. B* **1997**, *101*, 2678−2684.
(54) Vilan, A.; Ussyshkin, R.; Gartsman, K.; Cahen, D.; Naaman, R.; Shanzer, A. *J. Phys. Chem. B* **1998**, *102*, 3307−3309.
(55) Vilan, A. Ph.D. Thesis, Weizmann Institute of Science, 2002.

Table 1. Summary of the Dipole Moments for the Free dC−X Molecules and of the Electrical Effects (viz., CPD_L), Contact Angle (CA) of Water and Relative Integrated Intensities of the Carboxylate Binding Group Peaks at ∼1650 cm^{-1} [a] in Arbitrary Units (a.u.), and Relative Integrated F_{1s} XPS Intensities for These Molecules on Low- and High-Doped *n*-GaAs Surfaces

		Low-doped				High-doped			
molecule	dipole [D]	CPD_L [V]	CA[c]	FTIR × 10^4 [a.u.][b]	XPS[d]	CPD_L [V]	CA[b]	FTIR × 10^4 [a.u.][c]	XPS[d]
dC−OCH_3	−3.9	1.45 ± 0.12	34 ± 4°	3.3 ± 0.5	−	0.89 ± 0.02	22 ± 4°	4.5 ± 0.4	−
dC−CH_3	−2.9	1.16 ± 0.08	53 ± 4°	4.1 ± 0.5	−	0.88 ± 0.04	69 ± 4°	5.8 ± 0.5	−
dC−H	−2.0	1.05 ± 0.07	58 ± 2°	4.6 ± 0.4	−	0.86 ± 0.02	78 ± 5°	6.3 ± 0.7	−
bare	0.0	0.95 ± 0.03	19 ± 2°	−	−	0.64 ± 0.02	24 ± 3°	−	−
dC−CF_3	2.1	0.75 ± 0.03	60 ± 3°	3.7 ± 0.5	0.41 ± 0.05	0.47 ± 0.01	91 ± 4°	5.2 ± 0.4	0.55 ± 0.03
dC−CN	3.7	0.80 ± 0.02	61 ± 6°	3.9 ± 0.3	−	0.49 ± 0.01	49 ± 5°	5.0 ± 0.5	−

[a] We used the IR spectra of the molecularly modified n^+-GaAs or n^--GaAs after subtracting the spectra of the bare n^+-GaAs or n^--GaAs, respectively. [b] In general, the higher the coverage of molecules with hydrophobic terminations (i.e., H, CH_3, and CF_3) is, the higher the CA of water on the resulting surface. As shown in the table, bare *n*-GaAs is rather hydrophilic, more so than any of the other surfaces studied here. Therefore, the lower the molecular coverage, the higher is the hydrophilic contribution of bare *n*-GaAs domains and, therefore, the lower is the CA of water. As shown in the table, the CA for all hydrophobic terminations on high-doped GaAs is higher than that on low-doped GaAs, thus indicating higher molecular coverage on high-doped than on low-doped GaAs. For derivatives with polar terminations (i.e., CN and OCH_3), we cannot use the CA as an indication for coverage, because we cannot distinguish between a low CA due to low coverage (much bare GaAs exposed) or to high coverage. [c] The IR extinction coefficient for all derivatives was found to be the same, within the experimental error. [d] XPS measurements were performed only for the dC−CF_3 molecules because of the relative ease to detect the molecules via the F_{1s} signal. The values that appear in the table are the integrated intensities of the CF_3 concentrations, normalized to those of the Ga sites to which the carboxylate groups bind.[53]

2.4. Contact Potential Difference (CPD). CPD was measured in ambient conditions (293 K, 40% relative humidity) with a home-built system, based on a Besocke Kelvin probe, to determine the electrical potential of contact-free surfaces relative to that of a (Au) reference. For molecules on a semiconductor surface, the CPD reflects the work function of the surface, i.e., the electron affinity, χ_{sc}, plus the energy difference between the conduction band minimum and the Fermi level. The work function will vary with the potential drop, ΔV, over a surface dipole layer, which is a function of the molecule's dipole moment, μ,[56] according to:[22,57,58]

$$\Delta V = \frac{N \cdot \mu \cdot \cos\theta}{\epsilon\epsilon_0} \quad (1)$$

Here, N is the molecular density of the different derivatives; θ is the average tilt of molecules relative to the surface normal; ϵ is the effective dielectric constant of the molecular film (including any depolarization effects[59]); ϵ_0 is the permittivity of free space.[58]

The energies of the band at the semiconductor surface are normally shifted compared to their value in the bulk due to surface charges. This difference is the band bending (BB), which is taken positive for an *n*-type semiconductor with a depletion layer. These surface charges can be neutralized, and thus, the band bending can be eliminated by illumination with saturating supra-band gap radiation. The difference between this CPD value (CPD_L; the CPD value with the system near-flat band, i.e., BB → 0) and that obtained in the dark is the surface photovoltage (SPV). The reason that BB→ 0, under illumination and, indeed, is not pinned, stems from the binding of the dC−X molecules.[39,48,60] These molecules bind to the sites that otherwise would serve to create states that pin the Fermi level.[39,48,60]

2.5. X-ray Photoelectron Spectroscopy (XPS). Ex situ XPS measurements were carried out for samples modified with dC−CF_3 on an AXIS−HS Kratos instrument using monochromatized Al (K_α) X-rays ($h\nu$ = 1486.6 eV) and pass energies ranging from 20 to 80 eV. The resolution was ∼0.5 eV. Additional XPS and UV photoelectron spectroscopy (UPS) data on Au/dC−X/GaAs junction, germane to the formation of the Au contact by indirect evaporation, have been reported by us earlier.[42]

2.6. Contacts. Immediately following adsorption, Au or Pd was evaporated, indirectly, on the molecularly modified surfaces. For this, the molecularly modified surfaces were introduced into an electron-beam evaporator, *facing away* from the metal source.[32,36,42,51] Evaporation was started after reaching a base vacuum pressure of $4-6 \times 10^{-7}$ Torr and then refilling the chamber with Ar ($1.5-1.9 \times 10^{-3}$ Torr) and cooling the sample holder down to 150−200 K. This ensures that only metal atoms and clusters that scattered off Ar atoms or the chamber's walls reach the sample. The effective deposition rates of the Au and Pd atoms/clusters on top of the samples are estimated to be $6 \times 10^{-4}-2 \times 10^{-3}$ and $3-9 \times 10^{-3}$ nm/sec, respectively. For (photo) electrical measurements, 30 nm of Au was evaporated. The presence of a coldfinger, colder than the sample holder, kept condensation products from accumulating on the sample. For comparison, in specific experiments we employed "ready-made" contacts, using the "fast" version of the Lift-Off, Float-On (LOFO) of metal (Au or Pd) process, which was described in detail elsewhere.[38]

2.7. Electrical Characterization. Current−voltage ($I-V$) measurements were carried out with a Keithley 2400 source meter between −0.8 and +0.8 V in steps of 10 mV, in a vacuum ($1.0-1.5 \times 10^{-4}$ Torr) at temperatures between 200 and 295 K. The results were analyzed according to the thermionic emission model (cf. Supporting Information, section 2).[61] To this model, a double-Gaussian energy distribution of interface states was added (cf. section 4.3 for more details). For each junction the bias was applied between the Ohmic back contact, which was grounded, and the metal pad, contacted by a micromanipulator (Karl Suss).

Capacitance−Voltage ($C-V$) characteristics were recorded between −0.8 and +0.8 V DC bias, at 1 MHz, with an HP 4194 impedance analyzer. The data were analyzed according to the Mott−Schottky model (cf. section 4.4 below for more details; cf. Supporting Information, section 2).[61]

Internal photoemission (IPE) spectra were collected at zero bias in the 0.7−1.2 eV range, below the GaAs band gap (1.4 eV) absorption. The measurements were possible only for the low-doped samples because of too high dark currents for the high-doped samples (cf. Supporting Information, section 1c). The photon flux, modulated at 13 Hz, and the photocurrent response were measured using a *lock-in* amplifier.[62] The data were analyzed according to Fowler's equation[63−65]

(56) We use here as the relevant dipole moment that of the molecule bound to the GaAs surface, as calculated in ref 25, rather than the free molecule's dipole moment, as we did in earlier work. We note that, as noted also in ref 25, the general trends are very similar, reflecting the changes within the series of molecules with identical binding group.

(57) Moench, W. *Semiconductor surfaces and interfaces*, 3rd ed.; Springer-Verlag: Berlin, Germany, 2001.
(58) Bruening, M.; Moons, E.; Cahen, D.; Shanzer, A. *J. Phys. Chem.* **1995**, *99*, 8368−8373.
(59) Gershevitz, O.; Sukenik, C. N.; Ghabboun, J.; Cahen, D. *J. Am. Chem. Soc.* **2003**, *125*, 4730−4731.
(60) Cohen, R.; Bastide, S.; Cahen, D.; Libman, J.; Shanzer, A.; Rosenwaks, Y. *Adv. Mater.* **1997**, *9*, 746−749.
(61) Rhoderick, E. H. *Metal-semiconductor contacts*; Oxford University Press: London, U.K., 1978.
(62) Ishida, T.; Ikoma, H. *J. Appl. Phys.* **1993**, *74*, 3977−3982.

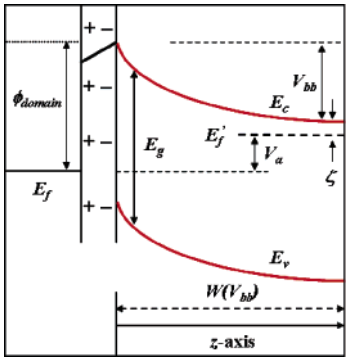

Figure 2. One electron energy (vertical axis) band diagram for metal/dipole layer/*n*-semiconductor junction with a negative layer dipole moment as a representative example. The diagram is drawn for the case where bias, represented by positive voltage V_a, is applied across the junction. E_f is the Fermi level of the metal, E_f' is the quasi-Fermi level of semiconductor, V_{bb} is the band bending corresponding to a junction with uniform Schottky Barrier Height (SBH) = ϕ_{domain}; $\zeta = (E_c - E_f')$. E_c and E_v are the bottom of the conduction and top of the valence band edges, respectively. Note that the thickness of the molecular layer ($d \approx 1$ nm) in the diagram is not properly scaled with respect to the thickness of depletion region, $W(V_{bb})$, which can be hundreds of nm for $V_a = 0$ V and a doping level, $N_d = 2 \times 10^{16}$ cm^{-3}.

and the parallel conduction model (cf. sections 4.2 and 4.3 below; cf. Supporting Information, section 1, for more details).

3. Theoretical Considerations

An energy band diagram of a metal/semiconductor junction under bias is shown in Figure 2, with a polar interfacial layer (left) depicting the molecular layer. For the analysis of the *I*−*V*, IPE, and *C*−*V* results, it is essential to consider the effect due to this interfacial layer. Furthermore, because the molecular layer is likely laterally inhomogeneous, the consequences of heterogeneity should also be considered. For simplicity, we shall only consider the first-order effect of inhomogeneity, viz. that of the molecular dipole layer at the interface containing pinholes or *perforations*. Therefore, transport data may need to be analyzed as arising from a mixture of the two following types of contacts:[51]

(1) direct metal−semiconductor contacts in the pinholes, characterized by a barrier height, $\phi_{pinhole}$, and

(2) metal−molecule−semiconductor contacts, characterized by a barrier height, ϕ_{domain}. Here, ϕ_{domain} specifically refers to the difference between the conduction band minimum (CBM) at the semiconductor−molecule interface and the Fermi level position in the metal (see Figure 2).

In this work, we are primarily interested in factors that control the transport in these mixed contacts and particularly the roles played by the molecular dipole moment and the extent of the layer inhomogeneity. To that end, we need to consider two separate issues concerning the present interfaces, namely: (1) the quantum mechanical transmission of carriers across the interface, and (2) the lateral variation of the Schottky barrier height (SBH).[61,66,67] The first issue, which is particular to interfaces with a molecular layer, arises because the quantum mechanical transmission of carriers across a molecular layer (arrow 1 in Figure 3) is typically orders of magnitude smaller

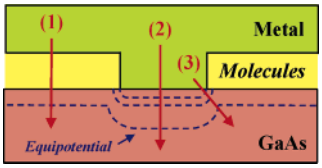

Figure 3. Potential distribution, not drawn to scale, near a pinhole in a molecular layer with a positive dipole moment ($\phi_{pinhole} > \phi_{domain}$). The electric field at the perimeter of the pinhole, e.g., along the path of arrow 3, is significantly higher than the electric field near the center of the pinhole, arrow 2.

than that across intimate metal−semiconductor interfaces (arrow 2 in Figure 3). An exception of this expected scenario is when the energy of the carriers corresponds to an energetic state of the interface molecule. The presence of molecular states within ~0.4 eV of the CBM of GaAs could lead to resonant transmission in the present experiment, because photoexcited electrons, with a maximum photon energy of 1.2 eV, have significant distribution in this energy range. It is unlikely that the molecules presently used have such low-lying molecular states because of the large LUMO−HOMO gaps.[25] Furthermore, when resonant states contribute to the carrier transport, the IPE spectrum is expected to reveal "plateaus". In the absence of such evidence, we shall assume that the transmission through the molecular layer in our samples is largely through tunneling and depends on the energy distribution of electrons that leave the metal (cf. Supporting Information, section 1c). Also, we shall assume that the probability for tunneling across the molecular domains is much less than that through pinholes (cf. Supporting Information, sections 1c and 4).

The second issue is common to all inhomogeneous interfaces, with or without the molecular layer. The potential distribution in the depletion region of the GaAs is governed by inhomogeneous boundary values at the interface ($\phi_{pinhole}$ and ϕ_{domain}) and, on the other end, by the equilibrium value in bulk semiconductor.[46,61,67] Poisson's equation can be used to solve for the potential distribution, for any specific applied bias.[46] Obviously, this boundary value problem is identical to problems of spatially inhomogeneous barrier heights previously solved for intimate metal/semiconductor junctions.[46,57] Those numerical solutions, which were shown to be accurately represented by a simple analytic "dipole layer approach"[68] and also to agree with experiment, can therefore be simply adopted for the present interfaces.[69] A major result from previous studies is the dependence of the effective barrier height on the lateral dimensions of the pinholes under certain conditions. When the lateral dimensions of a pinhole contact are greater than the depletion width, the carrier transport through the pinholes is not influenced by the molecular layer and the "effective" barrier height is simply the nominal barrier height, $\phi_{pinhole}$ (cf. cartoon

(63) Fowler, R. H. *Phys. Rev. B: Condens. Matter Mater. Phys.* **1931**, *38*, 45−56.
(64) Margaritondo, G. *Prog. Surf. Sci.* **1998**, *56*, 311−346.
(65) Okumura, T.; Tu, K. N. *J. Appl. Phys.* **1983**, *54*, 922−927.
(66) If a metal and a semiconductor are brought in electronic contact, an electrostatic potential barrier can form between them as a result of the flow of electrons between them to equilibrate their Fermi levels (the electrochemical potentials of the electrons). The result of this is a rectifying contact, described by the so-called Schottky−Mott model. The barrier is called a Schottky barrier. The height of this barrier is the Schottky Barrier Height (SBH).
(67) Sze, S. M. *Physics of semiconductor devices*, 2nd ed.; Wiley-Interscience: New York, 1981.
(68) Tung, R. T. *Phys. Rev. B: Condens. Matter Mater. Phys.* **1992**, *45*, 13509−13523.
(69) A short summary of the basic concepts of the "dipole layer approach" and the main results are provided in section 3 of the Supporting Information, which also contains a discussion of a minor modification that needs to be made for the boundary values bordering the molecular layer.

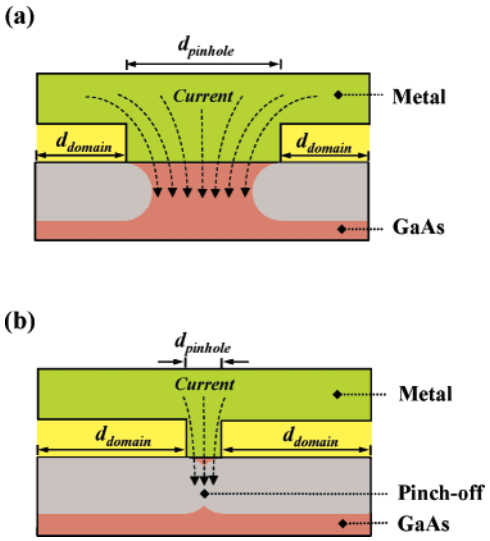

Figure 4. Scheme for illustrating the electrostatic potential of molecular domains on the conduction through adjacent pinholes, if (a) the dimension of pinholes, $d_{pinhole} > d_{domain}$ the molecular domain size and if (b) $d_{pinhole} < d_{domain}$.

of Figure 4a). The depletion width scales with and is typically a few times the Debye length of the semiconductor. We estimate that for GaAs with $N_d \approx 10^{16}$ cm^{-3}, the conduction through pinholes with diameters larger than their depletion region, viz. >30 nm, is not affected by the molecular dipole layer nearby (cf. Supporting Information, section 3.1, Figure 2S, and Table 1S). However, if the lateral inhomogeneity in the barrier height occurs on a length scale smaller than the semiconductor's depletion width, depletion regions will extend laterally in the semiconductor sufficiently so as to dampen the potential variations in the space charge region. The most pronounced effect of such extended space charge regions will be the apparent increase of the effective barrier height for regions with nominally low barrier height, due to the presence of high barrier height regions close by (cf. cartoon of Figure 4b). This effect, loosely termed "pinch-off", thus offers a mechanism by which the molecular layer may be used to control and tune the transport properties of the pinholes.

If the molecular layer introduces a positive dipole potential, i.e., $\phi_{domain} < \phi_{pinhole}$, the effective barrier height may be reduced. The reason is, though, different from that for the effective barrier increase with $\phi_{domain} > \phi_{pinhole}$. In the case of $\phi_{domain} < \phi_{pinhole}$, barrier lowering will occur under the edges of the large and small pinholes (as explained in more detail in Supporting Information, Section 3.2). To understand this, we can look at Figure 3. As illustrated by arrow 3 there, the edges of the pinholes are marked by an electric field that is significantly enhanced from that expected for a uniform diode (e.g. arrow 2 in Figure 3). This leads to enhanced field emission and leakage mechanisms that lower the apparent barrier height. As the pinhole size becomes smaller than the depletion width, the enhanced field emission is no longer limited to the edges of the pinhole but affects the entire pinhole region. An extreme case of this effect is analogous to field emission from sharp metallic filaments.

An additional issue that needs to be addressed is the high-frequency ac admittance of a mixed junction. It is well-known that the capacitance per unit area, C, of an intimate Schottky junction depends on the applied reverse bias, V_r, according to the Mott−Schottky relationship:[70]

$$\frac{1}{C^2} = 2 \times \frac{(V_{d0} - kT/q + V_r)}{q\epsilon_s N_d} = 2 \times \frac{(\phi_b - \zeta - kT/q + V_r)}{q\epsilon_s N_d} \quad (2)$$

where V_{d0} is the built-in potential in the semiconductor ($= (V_a + \zeta)$ in Figure 2), ζ is the doping-dependent position of Fermi level with respect to the conduction band edge in the bulk of semiconductor, and ϵ_s is the permittivity of the semiconductor.

When a dielectric layer, e.g., a molecular layer of thickness d_M and permittivity ϵ_M, is inserted at the interface, the junction capacitance, in the absence of interface states, becomes:

$$\frac{1}{C^2} = 2 \times \frac{(\phi_b - \zeta - kT/q + V_r)}{q\epsilon_s N_d}\left[1 - 4\left(\frac{\epsilon_s d_M}{\epsilon_M W}\right)2 + ...\right] \quad (3)$$

where W is the depletion width. Because d_M is no more than a few nanometers and $W > 100$ nm at reverse bias, the correction term in the square parenthesis is completely negligible. Therefore, the large-bias capacitances can be used to determine the barrier height as before, even in the presence of a molecular layer. When the interface has mixed contacts, the $C-V$ method should yield a barrier height that is the weighted average of the barrier height distribution. Note that the $C-V$ technique uses out-of-phase current and, therefore, is not at all affected by quantum mechanical transmission at the interface.

4.Results

4.1. Characterization of Contact-Free dC−X/*n*-GaAs Surfaces. n^--GaAs and n^+-GaAs surfaces were modified by forming molecular monolayers on them. We reported earlier some results on n^+-GaAs samples.[37,38,54,55] Those results and new ones are noted and used here primarily for comparative purposes. The effect of molecular termination on the n^--GaAs and n^+-GaAs surface was studied by measuring the contact angle (θ) of water (Table 1). The contact angles are relatively low (i.e., the film is relatively hydrophilic) compared to what can be obtained with long alkyl chains, because these molecules cannot form very dense monolayers for steric reasons.

Molecules with hydrophobic termination groups (i.e., CH_3, H, and CF_3) showed lower contact angle values on n^--GaAs, than on n^+-GaAs, consistent with lower coverage on n^--GaAs than on n^+-GaAs (cf. Table 1, footnote b). Because of the hydrophilic nature of the bare (ambient-exposed) GaAs surfaces, we cannot use the CA of surfaces modified with molecules with hydrophilic termination groups (i.e., OCH_3 and CN) to assess coverage (cf. Table 1, footnote b).

For those molecules, we rely on the FTIR measurements, which, for the hydrophobic molecules, correlate well with the CA results (Table 1). For each termination group, integrating the FTIR peak of the carboxylate (COO^-) binding group (at ~1650 cm^{-1}) showed higher absorption values on n^+-GaAs than on n^--GaAs.

XPS was performed on representative samples of dC−CF_3/n^--GaAs and dC−CF_3/n^+-GaAs (Table 1). The results show the F/Ga ratio (F from the CF_3 termination group) on n^--GaAs to be lower than that on n^+-GaAs, again indicating lower

(70) Werner, J. H.; Guettler, H. H. *J. Appl. Phys.* **1991**, *69*, 1522−1533.

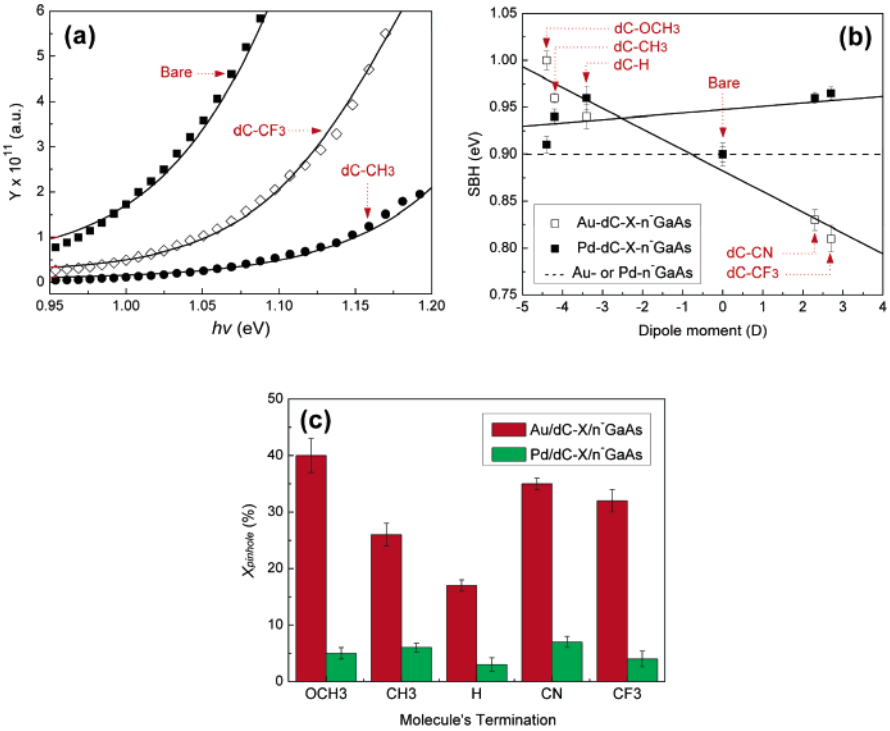

Figure 5. (a) Photoresponse yield (Y) vs photon energy ($h\nu$) at zero bias for Au/dC−X/n^--GaAs junctions, with negative dipole molecules (i.e., dC−CH_3), positive dipole molecules (i.e., dC−CF_3), and without molecules (i.e., bare) as representative samples. The smaller Y values for the molecularly modified junctions compared to those of the bare one are due to the molecular layer (because the photoexcited electrons need to cross the molecular layer; due to their short mean free path, even the very thin layer significantly increases the de-excitation probability). The solid lines are fits to the IPE data, using the PCM model with two barriers, (eq 5). For bare Au/ n^--GaAs junctions, the fit gives one barrier of 0.90 eV for 75% of the total area and one of 0.89 eV for 25% of the total area. For bare Pd/n^--GaAs junctions, the fit gives one barrier of 0.82 eV for 65% of the total area and one of 1.05 eV for 35% of the total area. The value given in Figure 5b is the weighted average of these two barrier heights (cf. Supporting Information, section 5). For molecularly modified junctions, the fits showed two barriers as shown in Figure 5b. (b) Dependence of IPE-derived SBHs of Au/ and Pd/dC−X/n^--GaAs junctions on the free molecule dipole moment. (c) Dependence of IPE-derived $X_{\text{pinhole}} = S_2/S_{\text{eff}}$ (cf. section 4.2), i.e., the fraction of the total area covered by pinholes, of Au/ and Pd/dC−X/n^--GaAs junctions on the termination groups of dC−X molecules. $X_{\text{pinhole}} = S_2/S_{\text{eff}}$ (cf. section 4.2), i.e., the fraction of the total area covered by pinholes. The two sets of data for each series of junctions are interpreted as originating from metal/GaAs and metal/dC−X/GaAs pinholes.

molecular coverage on n^--GaAs than on n^+-GaAs. Comparing XPS and FTIR measurements on n^--GaAs and n^+-GaAs by taking the CF_3/Ga ratios, i.e., $[(CF_3/Ga)_{n^-\text{-GaAs}}:(CF_3/Ga)_{n^+\text{-GaAs}}]$ (= 0.75), we find this ratio to correlate well with the ratio of FTIR intensities $[(COO)_{n^-\text{-GaAs}}:(COO)_{n^+\text{-GaAs}}]$ (= 0.71). The difference in adsorption on the two types of GaAs is explained in section 5.5.

The molecular effects on the electrical properties of the free surface were evaluated by measuring CPD and SPV, using the Kelvin probe. As shown in Table 1, the molecular layer modifies the CPD of both n^--GaAs and n^+-GaAs surfaces. For both doping levels, the effect correlates with the dipole moment of the (isolated) molecule; i.e., the two data sets show the same trend. Excluding the dC−OCH_3/n-GaAs, if we use the ratios of integrated FTIR intensities as a rough measure of relative coverage ($\propto N$ in eq 1 from section 3.4), we find an over-all stronger dipole effect on n^+-GaAs than on n^--GaAs.

For *all* dC−X molecules on high-doped GaAs, the *average* molecular effect on the CPD, viz. $|\Delta CPD_L/\Delta Dipole|$, is 0.07 V/D. For dC−$CH_3$, dC−H, dC−CN, and dC−$CF_3$ on low-doped GaAs, the average molecular effect is 0.05 V/D. The higher molecular effect on high-doped n-GaAs, compared to low-doped n-GaAs, is a direct indication for higher coverage of molecules on the surface. However, the effect of dC−OCH_3 on n^--GaAs is much higher, 0.21 and 3 times more than that on n^+-GaAs. A possible explanation is that in all other cases, the close distance between strong dipoles leads to dipole−dipole repulsion, which is decreased by depolarization.[71] In the case of the dC−OCH_3 compound, the lower coverage will decrease the dipole−dipole repulsion and, therefore, reduce or remove depolarization.[59] In section 5.5 we discuss the differences in molecular coverage on n^--GaAs and n^+-GaAs.

4.2. Internal Photoemission (IPE) Spectroscopy. IPE spectra are shown in Figure 5a. The spectra can be analyzed using Fowler formula:[63]

$$Y \propto (h\nu - q\phi_b)^2 \qquad (4)$$

where Y is the photoyield, i.e., the observed photocurrent per incident photon of energy, $h\nu$ (cf. Supporting Information, section 1c) and ϕ_b is the SBH. If the system has more than one barrier height, this will be reflected in the spectra.[64] Indeed, the IPE spectra show photocurrent onsets of the molecularly modified junctions that vary with the molecular dipoles (cf. Figure 5a and ref 51). Further analysis yields estimates for the fractions of the contact areas associated with the different barrier heights.

The photocurrent due to IPE yields the sum of currents due to different barriers, weighted according to their relative photoemission yields.[70] Because of the scattering of photogenerated electrons that reach the molecular layer from the metal, in IPE, the contribution of the metal−GaAs regions to the

(71) Shvarts, D.; Haran, A.; Benshafrut, R.; Cahen, D.; Naaman, R. *Chem. Phys. Lett.* **2002**, *354*, 349−353.

Table 2. Summary of the Relative Fraction of Pinholes, Γ,[a] Obtained from FTIR Data of Contact-Free dC−X/n^--GaAs (i.e., Γ^{FTIR}), Obtained from IPE Data of Au/ and Pd/dC−X/n^--GaAs Junctions (i.e., Γ^{IPE}), and the Normalized Difference between Them[b]

		Γ^{FTIR}	Γ^{IPE}		$\bar{\Gamma}$	
mol_1	mol_2	contact-free	Au	Pd	Au	Pd
dC−OCH_3	dC−CH_3	0.81 ± 0.04	0.81 ± 0.02	1.01 ± 0.06	0.00 ± 0.03	0.25 ± 0.05
	dC−H	0.73 ± 0.03	0.72 ± 0.04	0.98 ± 0.03	0.01 ± 0.02	0.34 ± 0.07
	dC−CN	0.86 ± 0.04	0.90 ± 0.04	1.02 ± 0.04	0.05 ± 0.01	0.19 ± 0.03
	dC−CF_3	0.89 ± 0.04	0.88 ± 0.02	0.99 ± 0.04	0.01 ± 0.02	0.11 ± 0.04
dC−CH_3	dC−H	0.89 ± 0.04	0.89 ± 0.04	0.97 ± 0.05	0.00 ± 0.01	0.09 ± 0.02
	dC−CN	1.05 ± 0.04	1.04 ± 0.04	1.01 ± 0.04	0.01 ± 0.02	0.04 ± 0.03
	dC−CF_3	1.09 ± 0.04	1.09 ± 0.05	0.98 ± 0.04	0.00 ± 0.01	0.10 ± 0.02
dC−H	dC−CN	1.18 ± 0.04	1.18 ± 0.04	1.04 ± 0.03	0.00 ± 0.02	0.12 ± 0.02
	dC−CF_3	1.23 ± 0.03	1.20 ± 0.04	1.01 ± 0.04	0.02 ± 0.02	0.18 ± 0.04
dC−CN	dC−CF_3	1.04 ± 0.03	0.96 ± 0.04	0.98 ± 0.04	0.05 ± 0.02	0.08 ± 0.02

[a] $\Gamma = (1 - X_{pinhole})_{mol_1}/(1 - X_{pinhole})_{mol_2}$; $X_{pinhole}$ = fraction of the contact area covered by Pinholes; mol_1 and mol_2 are two different dC derivatives. [b] $\bar{\Gamma} = |(\Gamma^{IPE} - \Gamma^{FTIR})/\Gamma^{FTIR}|$.

measured photocurrent is disproportionally larger than that of the molecular domains (cf. Supporting Information, section 1c).[64] To extract the SBH values of the molecularly modified junctions, we considered each IPE spectrum as the superposition of two contributions, each following Fowler's law:[65]

$$Y \propto \sum_{i=1,2} \frac{S_i}{S_{eff}}(h\nu - q\phi_{bi})^2 \qquad (5)$$

Here, S_{eff} is the total geometric area of the contact, and ϕ_{bi} and S_i are, respectively, the SBH and the area of regions 1 and 2, where $i = 1$ refers to the metal−dC−X−GaAs parts (molecular domains) and $i = 2$ to the metal−GaAs (pinhole) ones.[72] Fitting the IPE data with two SBHs yielded much better agreement with the raw experimental data than with only one SBH, whereas adding another barrier (fit to 3 SBHs) did not improve the fit. The SBHs extracted from the IPE data fall into two distinct classes (Figure 5b). The first type is almost the same for all types of junctions (0.88−0.91 eV for Au, and 0.89−0.90 eV for Pd), irrespective of the molecular properties. These values are similar to the weighted one obtained for the bare junctions (0.89 eV; cf. caption of Figure 5a and Supporting Information, section 5). Thus, we associate these values with the barrier at direct metal (M = Pd or Au)/GaAs contacts in the pinholes, i.e., ϕ_{b1} (= $\phi^{IPE}_{b,\,M-GaAs}$). The second type of barrier varies linearly with the dipole moment of dC−X, much stronger with Au than with Pd contacts (see section 5.3 for explanation). We associate this type with ϕ_{b2} (= $\phi^{IPE}_{b,\,M-dC-X-GaAs}$). Similar to what we reported earlier for such junctions with n^+-GaAs, using the current−voltage ($I-V$) technique,[36] the $\phi_{b,IPE}$ vs *dipole moment* trends of Pd/ and Au/dC−X/n^--GaAs junctions are opposite ones.

By fitting the IPE data to eq 5 we can extract the fraction of the total contact area covered by pinholes, $X^{IPE}_{pinhole} = S_2/S_{eff} = 1 - S_1/S_{eff}$, where $S_2 = S_{pinhole}$, the total area occupied by pinholes and S_{eff} is the total area of the contact that effectively contributes to the photocurrent. As shown in Figure 5c, the fraction of the contact area covered by pinholes is smaller for Pd/dC−X/n^--GaAs junctions than for the equivalent Au/dC−X/n^--GaAs ones. The question then is: to which degree these $X^{IPE}_{pinhole}$ values reflect the actual geometric fraction of pinholes in the monolayer?

For the type of junctions that we study here, we can use the IPE-extracted surface coverage as estimates, rather than for actual determination (cf. Supporting Information, sections 1c and 4). In fact, this holds for all the electrical characterization methods for metal/semiconductor junctions that we use here. Each of these has its pros and cons, and no one method will provide us with the "true" value. Therefore, to answer the question at the end of the previous paragraph, we need a nonelectrical estimate of $X_{pinhole}$. Such information can be obtained from the integrated intensities of the FTIR peaks at ~1650 cm^{-1} (Table 1), which give a measure of S_1. However, as these are not absolute values, we need to use *relative* $X_{pinhole}$ values, viz. $\Gamma = (S_1)_{mol1}/(S_2)_{mol2} = (1 - X_{pinhole})_{mol1}/(1 - X_{pinhole})_{mol2}$, for our comparison. Table 2 shows those values, from the FTIR measurements and from the $X^{IPE}_{pinhole}$ ones, i.e., it compares Γ^{IPE} with Γ^{FTIR}. Although there is no direct correlation between Γ and $X_{pinhole}$ (because $X_{pinhole}$ is a property of an individual monolayer whereas Γ is a property of one monolayer relative to another monolayer), the smaller is the normalized difference between Γ^{IPE} and Γ^{FTIR}, viz. $\bar{\Gamma} = |(\Gamma^{IPE} - \Gamma^{FTIR})/\Gamma^{FTIR}|$, the closer $X^{IPE}_{pinhole}$ is to the geometric value. As shown in Table 2, for Au/dC−X/n^--GaAs junctions $\bar{\Gamma} \cong 0$ within experimental error. In contrast, for Pd/dC−X/n^--GaAs junctions, $\bar{\Gamma}$ is mostly $\gg 0$. We ascribe these results to the inability of Pd to penetrate into small pinholes in the film, i.e., $X^{IPE}_{pinhole}$ values of Au/dC−X/n^--GaAs junctions reflect more reliably the fraction of contact area, taken up by pinholes in a monolayer than do the $X^{IPE}_{pinhole}$ values of the Pd/dC−X/n^--GaAs junctions (cf. discussion in section 5.4).

4.3. Current−Voltage ($I-V$) Measurements. In agreement with our earlier reports,[32,36,37,39] the $I-V$ characteristics of metal/dC−X/n^+-GaAs diodes vary systematically with the free molecule's dipole moment. This is reflected also in the effective SBH of these junctions, extracted from the $I-V$ curves at RT, in the 0.1−0.4 V bias region, using the thermionic emission model[61] (Figure 6), as shown below:

$$I = S \cdot A^* T^2 \exp\left(-\frac{(q\phi_b + q\Delta\phi_b)}{k_B T}\right) \cdot \left[\exp\left(\frac{qV}{nk_B T}\right) - 1\right] \qquad (6)$$

where I is the measured current, V is the applied bias, S is the actual geometric area of the diode (0.2 mm^2), A^* is the theoretical Richardson constant for n-GaAs (= 8.6 $A \cdot cm^{-2} \cdot K^{-2}$),

(72) Strictly speaking, $Y = T_1S_1(h\nu - q\phi_{b1}) + T_2S_2(h\nu - q\phi_{b2})$, where T is the transmission coefficient through the ith interface. Although we did refine the data to extract these two parameters, they are, not surprisingly, coupled. Such analysis showed smaller T than S variations between molecules.

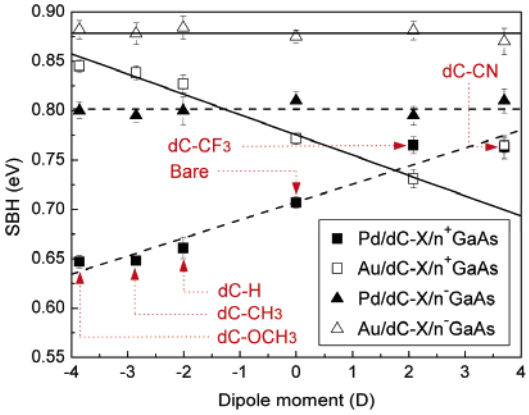

Figure 6. Dependence of effective SBH of metal/dC−X/n^--GaAs or metal/dC−X/n^+-GaAs junctions, derived from the experimental $I-V$ curves at RT, using the thermionic emission model in the 0.1−0.4 V bias region (with a theoretical Richardson constant of 8.6 A·cm^{-2}·K^{-2} for n-GaAs),[61] on the molecular dipoles of dicarboxylic acid derivatives. Dashed lines are fits to values for Pd-contacted junctions. Solid lines are fits to values for Au-contacted junctions. All results are for junctions made by indirect evaporation of the metal contacts.

q is the fundamental charge, n is the ideality factor, k_B is the Boltzmann constant and T is the temperature. $\Delta\phi_b$ is the image force lowering of the barrier height,[61] which was neglected in our earlier reports.[31,36,37,39,42,51]

The electrical effect of the different metals is clearly expressed in the series resistance, which is 100−200 times larger with Pd than with Au (Figure 7). The differences between Pd and Au are clear from the plots of the effective SBH values vs the free molecule dipole moment. These show a roughly linear but opposite correlation between molecular dipole and the junctions' SBH values (Figure 6; filled and open squares). *However, with n^--GaAs, we do not see any clear dependence on the free molecule's dipole moment, either in the raw $I-V$ data or if a single SBH for thermionic emission is assumed* (Figure 6; filled and open triangles), in agreement with earlier work.[55] The systematic molecular effects found for the Au/dC−X/n^+-GaAs junctions show that contacting does not significantly (if at all) damage the molecules below the metal contact.[32,36] Because the same contacting procedure (*indirect* evaporation) was used to contact the molecules on the n^+-GaAs and on the n^--GaAs, it is highly unlikely that the lack of dependence on molecular dipole is due to contact evaporation-induced damage, as is found if direct evaporation is used.[32]

In our preliminary communication, we showed that though $I-V$ measurements on metal/molecules/semiconductor diodes can be useful to estimate the electrostatic effects of homogeneous molecular layers, these measurements should be interpreted with care if the layer is inhomogeneous. The reason is that the current through the lower SBH domains dominates these measurements.[51] Therefore, we performed $I-V-T$ measurements on representative samples of the n^--GaAs junctions, i.e., Au/ or Pd/dC−CF_3/n^--GaAs and /dC−CH_3/n^--GaAs to test how far the experimental data indeed fit the physical picture of an inhomogeneous junction. As shown in Figure 7 for junctions with dC−CF_3 molecules, the results were well-behaved; i.e., for each metal, the ln(I) vs V slopes were similar to each other (in the 0.1−0.4 V bias region). At any given applied voltage, increasing the temperature increased the measured current in all junctions. The large amount of data obtained in the $I-V-T$ experiments then makes it possible to consider the junction as an inhomogeneous one and analyze it with a parallel conductance model (see below). For our analyses, we view the system as one with:

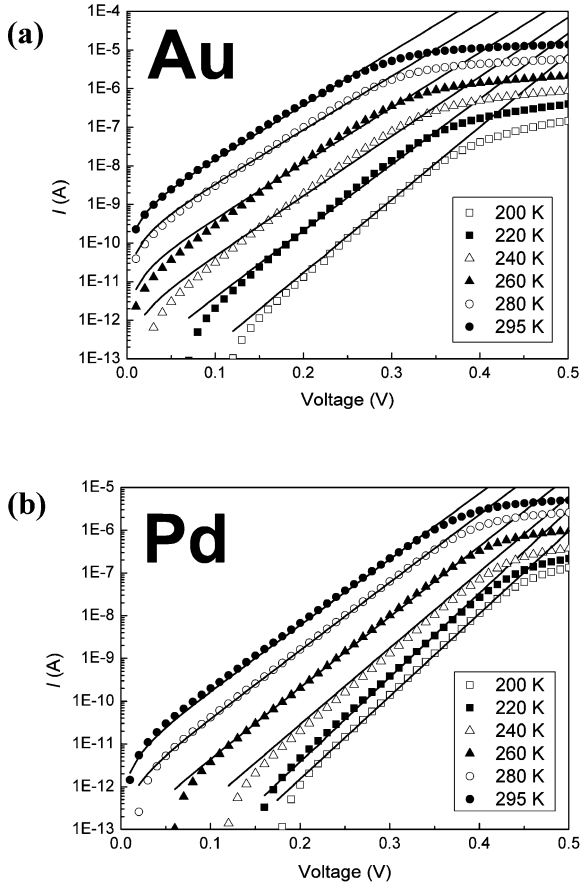

Figure 7. ln(*current*) − *voltage* (ln(I) −V) versus temperature of representative (a) Au/dC−CF_3/n^--GaAs and (b) Pd/dC−CF_3/n^--GaAs junctions in the range of 200−295 K. All results are for junctions made by indirect evaporation of the metal contacts. The continuous (black) lines are fits of the experimental data, using the double-Gaussian distribution model (eq 7). For all fits, $R^2 > 0.96$.

(i) Inhomogeneous distribution of metal-semiconductor contacts through large (2D) pinholes. As shown theoretically in section 3.2 of the Supporting Information, current through those pinholes is not influenced by the adjacent molecular domains.

(ii) Inhomogeneous distribution of metal−semiconductor contacts through small pinholes, i.e., defects with dimensions smaller than those of the surrounding molecular domains and defects in the molecular domains. Current through these pinholes and defects is influenced by the neighboring molecules (cf. Supporting Information, section 3.1 and Figure 2S).

(iii) Molecular domains: we neglect transport through the molecular domains, even if $\phi_{domain} < \phi_{pinhole}$, because of the additional tunnel barrier that will be involved for current via the molecular domains.[73,74] For the junctions used in this study, the electron transmission probability across the molecular domain is estimated, from calculations within the WKB tunneling model, to be <2.5% of that through the pinholes (cf. Supporting Information, section 3.2).

(73) Selzer, Y.; Salomon, A.; Cahen, D. *J. Phys. Chem. B* **2002**, *106*, 10432−10439.
(74) Selzer, Y.; Cahen, D. *Adv. Mater.* **2001**, *13*, 508−511.

Table 3. Summary of Results from $I-V-T$ Analysis of Metal/Molecule/n^--GaAs Junctions with Double-Gaussian Energy Distribution of Schottky Barrier Heights Using the Interface Dipole Layer Approach[68,92] by Fitting $\ln(I_S)$ vs. $(1/k_BT)$ Plots to Eq 7

Indirect Evaporation

contact deposition →	metal–GaAs in large pinholes[a]			metal–GaAs in small pinholes[b]		
junction ↓	ϕ_{b1} (eV)	f_1[c]	κ_1 (eV)	ϕ_{b2} (eV)	f_2[d]	κ_2 (eV)
Au/dC−CH_3/n^--GaAs	0.89 ± 0.01	2.4	0.01	0.96 ± 0.05	1.8	0.04
Au/n^--GaAs	0.89[e]	2.2	0.01[f]	–	–	–
Au/dC−CF_3/n^--GaAs	0.89 ± 0.01	2.2	0.01	0.83 ± 0.04	1.0	0.05
Pd/dC−CH_3/n^--GaAs	0.84 ± 0.02	2.0	0.02	0.79 ± 0.01	1.4	0.01
Pd/n^--GaAs	0.84[g]	2.0	0.04[h]	–	–	–
Pd/dC−CF_3/n^--GaAs	0.84 ± 0.02	2.0	0.02	0.87 ± 0.01	0.9	0.01

(fast) LOFO

contact deposition →	metal–GaAs in large pinholes[a]			metal–GaAs in small pinholes[b]		
junction ↓	ϕ_{b1} (eV)	f_1[c]	κ_1 (eV)	ϕ_{b2} (eV)	f_2[d]	κ_2 (eV)
Au/dC−CH_3/n^--GaAs	0.92 ± 0.03	0.68	0.03	0.88 ± 0.05	0.34	0.02
Au/ n^--GaAs	0.92	0.74	0.03	–	–	–
Au/dC−CF_3/ n^--GaAs	0.92 ± 0.03	0.69	0.03	0.95 ± 0.06	0.24	0.02
Pd/dC−CH_3/ n^--GaAs	0.91 ± 0.02	0.70	0.03	0.87 ± 0.01	0.21	0.02
Pd/ n^--GaAs	0.91	0.78	0.03	–	–	–
Pd/dC−CF_3/ n^--GaAs	0.91 ± 0.02	0.71	0.03	0.93 ± 0.01	0.23	0.02

[a] Large pinholes: defect areas in the molecular layer larger than the areas of the surrounding molecular domains. [b] Small pinholes: pinholes smaller than the surrounding molecular domains as well as defects in the molecular domains. [c] f_1: ratio between the effective and geometrical areas at metal/GaAs pinholes that are not pinched-off. [d] f_2: ratio between the effective and geometrical areas at the pinched-off metal/GaAs pinholes (which are molecule-controlled). [e] Weighted average of the two SBH values, obtained from the analysis: 0.90 eV for 70%, 0.88 eV for 30% of the interface. [f] The κ_i values were 0.01 eV for both SBH values. [g] Weighted average over two SBH values, obtained from the analysis: 0.74 eV for 60%, 1.01 eV for 40% of the interface. [h] Weighted average over the two κ_i values, obtained from the analysis: 0.02 eV for 60%, 0.08 eV for 40% of the interface.

Preliminary STM-based Ballistic Electron Emission Microscopy (BEEM) studies on representative Au/dC−X/*n*-GaAs samples support this view of the junction.[75]

With these assumptions in mind, we adapted a model that combines both the effects of dipole layer domains and the so-called parallel conduction model (PCM),[51,76] which, originally, assumes a (weighted) parallel connection between the different Schottky diodes, having discrete SBHs. This result is a model that can take into account any inhomogeneous distribution of both large and small pinhole metal−semiconductor contacts:

$$I = S \cdot A^* T^2 \sum_{i=1}^{2} f_i \cdot \exp\left(\frac{\kappa_i \cdot V_{bbi}^{\xi_i}}{(k_BT)^2} - \frac{\phi_{bi} - \Delta\phi_{bi}}{k_BT}\right) \cdot \left[\exp\left(\frac{qV}{k_BT}\right) - 1\right] \quad (7)$$

Terms with subscript $i = 1$ refer to large metal/GaAs pinholes that are not pinched-off, whereas those with $i = 2$, refer to small, pinched-off metal/GaAs pinholes that are molecule-controlled; f_i is the ratio between the effective and geometrical areas at zero bias; ϕ_{bi} and $\Delta\phi_{bi}$ are the SBHs and the corresponding image force lowering[61] for region i, V_{bbi} is the fitted band bending in region i, κ_i is the standard deviation of the Gaussian energy distribution of the SBHs,[77] ξ_i is a parameter that depends on pinhole geometry (mostly $\xi = 1/6$, except for molecule-free Au/ n^--GaAs junctions, where $\xi = 2/3$).[68,78] Fitting the $I-V-T$ data with three SBH (i.e., using eq 7, with $i = 1-3$), did not improve the fit we obtained with two SBHs.

Table 3 and Figure 8 summarize the results of the fit of the data to eq 7. The fits gave $R^2 > 0.96$. Although there is no molecular effect for the SBHs of the large pinholes ($i = 1$), clear trends with molecular dipole were observed for those of the small defects ($i = 2$). These trends are opposite for evaporated Au and Pd contacts. Results with Au and Pd contacts prepared by LOFO,[38,79] for comparison, show a systematic molecular effect similar to that obtained for the evaporated Pd/dC−X/n^--GaAs junctions (Table 3; Figure 8b). The ranges of the molecular effects for Pd- and Au-LOFO junctions were comparable to each other but lower than those for junctions contacted by evaporation. This is consistent with the higher f_2 values (i.e., the ratio between the effective and geometrical areas of the pinched-off metal/GaAs pinholes that are molecule-controlled) for evaporated contacts than for LOFO ones. The dependence of f_2 and f_1 (i.e., the ratios between the effective and geometrical areas of the metal/GaAs pinholes that are pinched-off and those that are not pinched-off, respectively) on the contacting method (evaporation vs LOFO) as well as on the contacting metal (Pd vs Au) will be discussed in sections 5.3 and 5.4 in terms of concentrations of large and small pinholes at the metal/semiconductor interface and morphology effects of the different contacts.

4.4. High-Frequency Capacitance−Voltage ($C-V$) Measurements. High-frequency $C-V$ data depend on the diffusion voltage and donor density (cf. Supporting Information, section

(75) Marginean, C.; Tivarus, C.; Haick, H.; Cahen, D.; Pelz, J. P. Unpublished results.
(76) Ohdomari, I.; Tu, K. N. *J. App. Phys.* **1980**, *51*, 3735−3739.
(77) $\kappa_i = \sigma_i^2/[2(\epsilon_s/q\,N_d)^{\xi}]$ with σ_i is the standard deviation of the Gaussian energy distribution, ϵ_s is the permittivity of the semiconductor, q is the electron charge, N_d is the doping density, and ξ is defined in the following footnote.
(78) ξ is a measure of the geometry of SBH variation and is determined empirically by fitting the functional form of the experimentally observed currents. Theoretically, it was found that SBHs with circular or stripe geometries that are homogeneously distributed at the interface have $\xi = 2/3$ or $\xi = 1/2$, respectively. The lower are the ξ values that are obtained by fitting the functional form of the experimentally observed currents, the higher is the SBH variation, i.e., the larger is the degree of inhomogeneity. We find $\xi = 1/6$, which indicates a high degree of inhomogeneity, relative to the ideal case.
(79) In contrast to what is the case with vacuum evaporation, with LOFO it is extremely unlikely that any diffusion of the metal will occur through the organic monolayer.

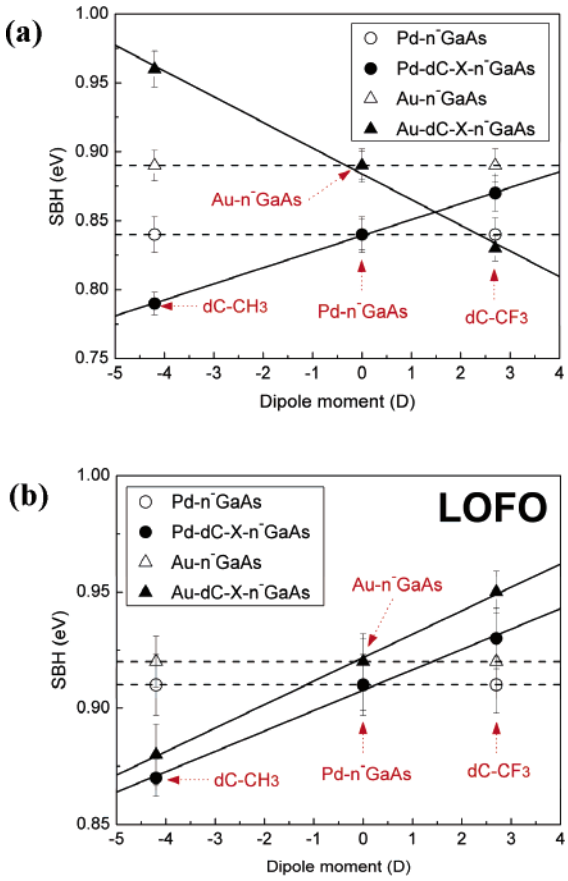

Figure 8. Dependence of SBH of metal/dC−X/n^-GaAs and metal/n^--GaAs regions, derived from $I-V-T$ data, by fitting a double-Gaussian energy distribution of SBHs model to the data on the molecular dipoles of the dicarboxylic acid derivatives for junctions contacted by (a) indirect evaporation and (b) fast LOFO.[38] The lines are fits to the barrier values that do (—) and do not (- - -) show a dependence on molecule type.

1b) and will, therefore, ideally correspond to the average SBH of the entire contact, with little effect of image-force lowering (in contrast to what is the case for $I-V$ measurements). This is reflected also in the effective SBH of these junctions, found by fitting the $C-V$ data to the general Mott−Schottky relationship (eq 2).[80]

Analyzing the Pd/ and Au/dC−X/n^+-GaAs $C-V$ data with eq 2 shows a reasonable *SBH* vs *molecular dipole* trend similar to those obtained from IPE and $I-V$ measurements (Table 4). In contrast, $C-V$ measurements performed on Pd/ and Au/dC−X/n^--GaAs show no correlation with the molecular dipoles. Therefore, we analyzed these $C-V$ data using the parallel conduction model. According to this model, the total junction capacitance equals the sum of the capacitances of the bare (NOTE: The capacitance measurement does not distinguish between pinched-off and not pinched-off bare regions; cf. ref 81.) and molecularly modified regions at the interface and is dominated by the type that occupies the largest interface area. To adapt this model to our experimental $C-V$ results, we considered a configuration with two parallel capacitors:[51]

$$S \cdot C = \sum_{i=1,2} S_i \frac{q\epsilon_s N_d}{2(\phi_{bi} - \zeta - kT/q + V_r)} \qquad (8)$$

where S is the geometric area, ϕ_b from eq 2 was replaced by ϕ_{bi}, as it refers to the SBH of the specific region with geometric area S_i, rather than of the whole contact area and all other symbols were defined earlier in eq 2.[80] Theoretically, eq 8 will give precise results only if the dimensions of all pinholes are well over the depletion width of the semiconductor (>100 nm for n^--GaAs). Because it is likely that Au/dC−X/n^--GaAs junctions contain both smaller pinholes and larger ones (than the n^--GaAs depletion width), eq 8 can yield only estimates of the various SBHs at the interface. Because of this, use of the PCM to analyze the high-frequency $C-V$ data will yield less-precise results than analyzing IPE results with the PCM (eq 5) and $I-V$ data with the double-Gaussian distribution model (eq 7).

Within eq 8, the best fit that we obtain for the molecularly modified junctions, is with two, rather than three SBHs.[81] All fits were with $R^2 > 0.95$. For all samples contacted by Pd or Au, the first SBH (ϕ_{b1}), is nearly constant and similar to the value found for the bare Pd/ or Au/n^--GaAs junction (see Figure 9 and Table 4). Therefore, we attribute ϕ_{b1} to direct metal/n^--GaAs contacts through pinholes in the Pd/ and Au/dC−X/n^--GaAs junctions. The second SBH (ϕ_{b2}) depends on the molecular dipole moments of the free molecules as well as on the contacting metal (Figure 9) and is attributed to the (semiconductor below the) molecular domains. Mostly, the molecular trends extracted from the $C-V$ data by the parallel conduction model were consistent with those from IPE and $I-V$, except for the results obtained from fitting the $C-V$ data of Pd/dC−X/n^--GaAs to the PCM. These show smaller barriers for the direct, molecule-independent contacts, ϕ_{b1}, than for the molecule-dependent ones, ϕ_{b2}. These observations are ascribed to growth morphology of the Pd contacts, as will be discussed in section 5.3.

In Table 4 we give also the $C-V$-derived fraction of pinholes ($X_{pinhole}$) and the ratio between the effective and geometrical contact areas (S_{eff}) (cf. Supporting Information, section 1).

5. Discussion

5.1. Comparison between SBHs of Different Bare Metal/*n*-GaAs Junctions. Differences are found between barrier heights for Au- and Pd-contacted junctions, extracted from $C-V$ and $I-V$ measurements for the n^+-GaAs samples, and from $I-V$, $C-V$, and IPE measurements for the n^--GaAs samples. Whereas the barrier heights of Au/n^--GaAs junctions extracted from $I-V$ and $C-V$ are comparable to those derived from the IPE data, those for Pd/n^--GaAs junctions are lower. For a given measure-

(80) Assuming $\epsilon_{mol} = 4$ and a molecular layer thickness of 1 nm, the capacitance of the molecular film per unit (C_{mol}) area is $\sim 4 \times 10^{-6}$ F/cm^2. Assuming capacitors that are connected in series, the corresponding $1/C_{mol}$ is negligible compared to the $1/C_d$ of the low-doped *n*-GaAs at zero bias ($C_d \approx 5 \times 10^{-8}$ F/cm^2) and, as $1/C = 1/C_{mol} + 1/C_d$, with $C_{mol} \gg C_d$ then $1/C \approx 1/C_d$.

(81) In metal/dC−X/*n*-GaAs junctions, there are basically three types of SBH: (1) metal/dC−X/*n*-GaAs; (2) nonpinched-off metal/*n*-GaAs (i.e., large 2D pinholes); and (3) pinched-off metal/*n*-GaAs (i.e., small pinholes). However, $C-V$ measurements cannot distinguish between pinched-off and non-pinched-off domains. This can be understood as follows. The capacitance at a given voltage is essentially determined by the depletion width at that voltage, which is determined by the average conduction band energy at the GaAs interface, the doping density in the GaAs, and the Fermi energy in the bulk of the GaAs. The detailed shape of the conduction band in the depletion region makes little difference, because there are no free carriers there anyway. This is why image force effects are not important, as pointed out in refs 46 and 61. In this case, it does not matter whether there are pinched-off points or not in the depletion region. Because that is so, the analysis of the $C-V$ data can be used only to distinguish between large metal−GaAs pinholes and metal−molecules−GaAs domains.

Table 4. SBH Values of Evaporated Metal/dC−X/*n*-GaAs (high- and low-doped) Contacts, as Derived from 1 MHz Capacitance-voltage Data using the normal Mott−Schottky Model and with the Parallel Conduction Model (PCM)[a]

Mott−Schottky

		n^+-GaAs		n^--GaAs	
		Au	Pd	Au	Pd
mol	dipole	ϕ_b (eV)	ϕ_b (eV)	ϕ_b (eV)	ϕ_b (eV)
dC−OCH_3	−3.9	0.97 ± 0.04	0.43 ± 0.04	1.11 ± 0.05	1.07 ± 0.06
dC−CH_3	−2.9	1.05 ± 0.03	0.68 ± 0.03	1.06 ± 0.03	1.00 ± 0.05
dC−H	−2.0	0.93 ± 0.03	0.53 ± 0.03	1.12 ± 0.05	1.03 ± 0.03
bare	0.0	0.84 ± 0.02	0.65 ± 0.03	1.12 ± 0.04[b]	0.98 ± 0.03[b]
dC−CF_3	2.1	0.63 ± 0.03	0.88 ± 0.03	1.11 ± 0.04	1.09 ± 0.05
dC−CN	3.7	0.71 ± 0.02	0.71 ± 0.05	1.06 ± 0.03	1.07 ± 0.04

C−*V* Parallel Conduction Model

		n^--GaAs							
		Au				Pd			
mol	dipole	ϕ_{b1} (eV)	ϕ_{b2} (eV)	$X_{pinhole,C-V}$ (%)	S_{eff}/S_{geom}	ϕ_{b1} (eV)	ϕ_{b2} (eV)	$X_{pinhole,C-V}$ (%)	S_{eff}/S_{geom}
dC−OCH_3	−3.9	0.91 ± 0.03	1.21 ± 0.04	44	1.44	0.88 ± 0.03	1.07 ± 0.03	21	1.57
dC−CH_3	−2.9	0.91 ± 0.03	1.14 ± 0.05	41	1.41	0.88 ± 0.02	1.08 ± 0.02	22	1.62
dC−H	−2.0	0.90 ± 0.03	1.20 ± 0.03	32	1.32	0.88 ± 0.04	1.10 ± 0.04	18	1.74
bare	0.0	−	0.89[c]	−	1.57	−	0.87[d]	−	1.95
dC−CF_3	2.1	0.89 ± 0.03	0.80 ± 0.05	6	1.38	0.88 ± 0.02	1.15 ± 0.03	15	1.56
dC−CN	3.7	0.89 ± 0.03	0.78 ± 0.05	4	1.23	0.88 ± 0.03	1.16 ± 0.02	15	1.54

[a] With the PCM, both the direct metal/*n*-GaAs contacts SBH values (ϕ_{b1}), and those through the molecular films (ϕ_{b2}) are derived, with $R^2 > 0.95$. The relative contribution of leakage to the experimental *C*−*V* characteristics ($X_{pinhole,C-V}$), as well as the ratio between the effective area (S_{eff}) and the geometric one (S_{geom}) for these junctions, as derived from the model, are also given. [b] The higher SBH values extracted by the Mott−Schottky model than those found with the *C*−*V* parallel conduction model stem from "leakage" in the system, probably due to the back-Ohmic contact. This leakage increases the SBH that is extracted from the data, compared to a system without leakage. Whereas the Mott−Schottky model does not take this leakage into account, the *C*−*V* parallel conduction model does. [c] The *C*−*V* PCM for bare Au/n^--GaAs showed two SBHs (0.91 eV for 70% of the total area and 0.87 eV for 30% of the total area) with a weighted average of 0.89 eV (cf. Supporting Information, section 5). [d] The *C*−*V* PCM for bare Pd/n^--GaAs showed two SBHs (0.83 eV for 70% and 0.96 eV for 30% of the interface) with a weighted average of 0.87 eV (cf. Supporting Information, section 5).

ment technique, the decrease in SBH values of metal/n^+-GaAs as compared to /n^--GaAs junctions can be ascribed to a shift of the bulk Fermi level toward the bottom of the conduction band (cf. Experimental Section). In section 5 of the Supporting Information, we show that the differences between SBHs extracted by the various techniques for metal/n^+-GaAs, as well as between those and the values for metal/n^--GaAs junctions, can be explained by interface heterogeneity because of oxides.

Our data are consistent with higher reactivity toward GaAs of evaporated Pd than Au. Furthermore, whereas Au forms complexes with oxides on GaAs,[82−84] Pd reacts with these oxides and, in some cases, "disperses" them on the metal/semiconductor junction.[85,86] Because Au diffuses readily, also through tens-of-nm GaAs-oxide layers,[82,87] i.e., significantly thicker than the 1−2 nm of oxide found on our n^--GaAs substrates,[39,42] the Au/oxide/GaAs surface will be relatively homogeneous, in agreement with an earlier report.[88] In the Pd/n^--GaAs junctions, both Pd/GaAs/oxide/n^--GaAs and direct Pd/n^--GaAs contacts can coexist. Thus, with Au as contact, a relatively homogeneous Au/oxide/GaAs system results, whereas with Pd, a more heterogeneous system is left.

What the various comparisons between all these data show most clearly is the importance of using systematically varying series of samples to look for true molecular effects, because of the problems of comparing single systems with and without molecules, as will be discussed in the next section. Although in our case part of the "problem" is because we consciously chose to work in ambient atmosphere (to show that molecular control can be achieved even under these conditions), the approach is valuable also if working in inert atmosphere or vacuum.

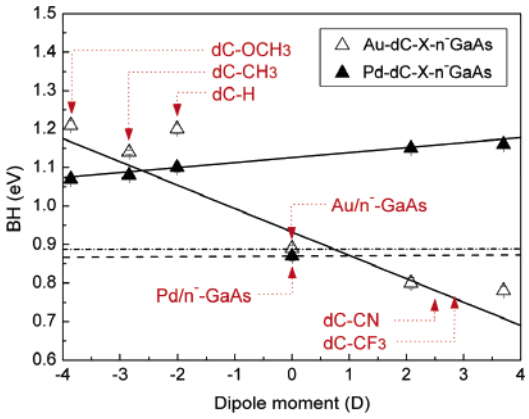

Figure 9. Dependence of SBH, derived from high-frequency *C*−*V* data and analyzed within the parallel conduction model of metal/dC−X/n^--GaAs and metal/n^--GaAs regions, on the molecular dipoles of dicarboxylic acid derivatives for junctions contacted by indirect evaporation. The lines are fits to the barrier values that do (—) and do not (- - - - and -•-•-•) show a dependence on molecule type.

(82) Weizer, V. G.; Fatemi, N. S. *J. App. Phys.* **1988**, *64*, 4618−4623.
(83) Persson, A. I.; Larsson, M. W.; Stenstroem, S.; Ohlsson, B. J.; Samuelson, L.; Wallenberg, L. R. *Nat. Mater.* **2004**, *3*, 677−681.
(84) Gupta, R. P.; Khokle, W. S.; Wuerfl, J.; Hartnagel, H. L. *Thin Solid Films* **1987**, *151*, L121−L125.
(85) Yablonovitch, E.; Sands, T.; Hwang, D. M.; Schnitzer, I.; Gmitter, T. J.; Shastry, S. K.; Hill, D. S.; Fan, J. C. C. *Appl. Phys. Lett.* **1991**, *59*, 3159−3161.
(86) Chor, E. F.; Zhang, D.; Gong, H.; Chong, W. K.; Ong, S. Y. *J. Appl. Phys.* **2000**, *87*, 2437−2444.
(87) Bonapasta, A. A.; Buda, F. *Phys. Rev. B: Condens. Matter Mater. Phys.* **2002**, *65*, 045308/1−045308/9.
(88) Chang, S.; Raisanen, A.; Brillson, L. J.; Shaw, J. L.; Kirchner, P. D.; Pettit, G. D.; Woodall, J. M. *J. Vac. Sci. Technol., B* **1992**, *10*, 1932−1939.

5.2. Effect of dC−X Molecules on Metal/*n*-GaAs SBHs. Why Do We See any Molecular Effect? Figures 5, 6, 8, and 9 and Tables 3 and 4 clearly show that the SBHs of Au/ and Pd/*n*-GaAs junctions are affected by the presence of the dC−X molecules at the interface also if low-doped GaAs is used. This feature, though seen directly from the IPE spectra (Figure 5a), becomes clear from the *I*−*V*−*T* and *C*−*V* data only after we use the parallel conduction model to analyze those data, i.e., take into account that the junctions are strongly heterogeneous. The primary reason for this inhomogeneity is that, because of their size and shape, dC−X molecules form incomplete monolayers on both n^--GaAs and n^+-GaAs.[48,89] This is supported by our XPS data, which show that the ratio CF_3/Ga < 1 (Table 1), and from our time-of-flight secondary ion mass spectroscopy (TOF SIMS) results.[42] The reason for the differences observed between n^--GaAs and n^+-GaAs (cf. Figure 6) will be discussed in section 5.5.

Contacting the molecularly modified surfaces by metal evaporation results in direct metal/GaAs and metal/molecule/GaAs contacts (cf. section 4.3, third paragraph).[32,36,42,51,90,91] Unless $\phi_{domain} \ll \phi_{pinhole}$, the necessity of tunneling will make transport via the domains less favorable than transport through the pinholes (cf. Supporting Information, section 3.2).[37,39] Therefore, one could argue that the molecules affect electron transport across the barrier simply by the extent of their coverage, viz., by the area that they leave for direct semiconductor/metal contact. In such a scenario, they would only serve as a current blocker. For this to be true, we expect the molecular effect per unit area in the metal/dC−X/*n*-GaAs domains of the different junctions to be constant. However, from our experimental IPE data, we extract barrier heights for molecular domains formed by the different molecules that are different. These differences are without any correlation with the differences in coverage as obtained from the FTIR results on n^--GaAs (Table 1). Similar conclusions can be drawn for the metal/dC−X/n^--GaAs barriers deduced from *I*−*V* and *C*−*V* measurements. Therefore, the molecular effects we derive from analyzing the data for the n^--GaAs samples (in terms of parallel conduction) are attributed primarily to an active electrical role of the molecules at the interface, rather than to the extent of their coverage on the GaAs surface and/or different effective areas of the metal contacts.

How Do the Molecules Affect the Junction Characteristics? We conclude that domains of monolayers of these dipolar molecules influence, by way of their electrostatic effect ***in*** the semiconductor, the electronic properties of the junctions. They do so by affecting the semiconductor below the areas where there are no molecules, the pinholes (cf. cartoons of Figure 4). The reason is pinching-off of low barrier height regions by higher barrier height ones,[68,92] as explained in the theoretical section and section 3.2 of the Supporting Information. Because of the heterogeneity of the resulting interface, we need the parallel conduction model to analyze the data with, in the case of the *I*−*V*−*T* data, a double-Gaussian energy distribution of barriers. With such analyses, the molecular effect is clear for all junctions and with all methods. There are, however, differences between the SBHs as deduced by the different methods,[45] and those will be discussed briefly.

Because in *I*−*V* measurements transport through the molecular domains will be negligible (unless $\phi_{domain} \ll \phi_{pinhole}$), current will not flow through these domains and the technique will not be sensitive to the barriers under those domains. The *I*−*V* results will, thus, reflect primarily current flow through pinholes and will be weighted in favor of lower barrier height regions. In contrast to *I*−*V*, in IPE, electrons come from states in the metal well above the Fermi level. The higher transmission probability at these higher energies means that electrons can, to some extent, pass through the molecular domain. Therefore, with IPE, we can also measure the electronic properties (i.e., SBH) below the molecular domains directly. However, the presence of the molecules decreases the yield of photoelectrons, underestimating the contact area (see Supporting Information, section 1c). In contrast to these, *C*−*V* probes the diffusion voltage of the semiconductor below both the pinholes and molecular domains without the need for carrier transport across the junction. Therefore, the results are not weighted in favor of the lower barrier height pinholes.[46,68,92] Because of these differences, *C*−*V* will give SBH values with stronger dipole effects than those relevant for charge transport in *I*−*V* and IPE in these junctions.[45,93,94] Still, this is of interest as from the differences we can learn about the molecular effect on the semiconductor below molecular domains. Then, for junctions contacted by different metals, comparing the results obtained by IPE, *I*−*V*, and *C*−*V* can indicate the contributions of each part of the junction (i.e., in the case of these junctions, the contributions of small and large pinholes and of molecular domains).

Further evidence for this interpretation of the molecular effects on the metal/semiconductor interface comes from comparing results with molecules that have opposite dipoles. Those should affect the bare junction oppositely, relative to the unmodified junction.[26,39] Especially, what we derive from our *I*−*V* results for Pd/dC−X /n^--GaAs junctions and from *I*−*V*, *C*−*V*, and IPE for Au/dC−X/n^--GaAs junctions fit this expectation (cf. last two paragraphs in section 5.4).

Results of studies on metal/GaAs junctions with molecular coverages between 40 and 98% (by adsorbing different mixtures of dC−X and benzoic acids) and on metal/Si junctions, with molecular coverages between 10 and 99% (by adsorbing molecules similar to those used in refs 59 and 95), support the dominant role of direct metal−semiconductor contacts via pinholes in controlling barrier heights for a broad range metal/monolayer/semiconductor junctions.[96] Changes in molecular coverage on these surfaces affect electronic transport through the junctions in a highly nonlinear fashion, consistent with the conclusions drawn from the work presented here.

Effect of Oxide at Interface. Still, the absolute SBH values for Pd/dC−X/n^--GaAs junctions derived from the *C*−*V* data are not explained by the arguments brought here. Although the differences *between* Pd/dC−X/n^--GaAs junctions with the

(89) Vilan, A.; Ussyshkin, R.; Gartsman, K.; Cahen, D.; Naaman, R.; Shanzer, A. *J. Phys. Chem. B* **1998**, *102*, 3307−3309.
(90) Walker, A. V.; Tighe, T. B.; Cabarcos, O. M.; Reinard, M. D.; Haynie, B. C.; Uppili, S.; Winograd, N.; Allara, D. L. *J. Am. Chem. Soc.* **2004**, *126*, 3954−3963.
(91) Haynie, B. C.; Walker, A. V.; Tighe, T. B.; Allara, D. L.; Winograd, N. *Appl. Surf. Sci.* **2003**, *203*−*204*, 433−436.
(92) Tung, R. T. *Appl. Phys. Lett.* **1991**, *58*, 2821−2823.
(93) Freeouf, J. L.; Jackson, T. N.; Laux, S. E.; Woodall, J. M. *J. Vacu. Sci. Technol.* **1982**, *21*, 570−573.
(94) Okumura, T.; Tu, K. N. *J. Appl. Phys.* **1987**, *61*, 2955−2961.
(95) Gershewitz, O.; Grinstein, M.; Sukenik, C. N.; Regev, K.; Ghabboun, J.; Cahen, D. *J. Phys. Chem. B* **2004**, *108*, 664−672.
(96) Haick, H. et al. and Azulay, D. et al. To be published.

different molecules agree qualitatively with those obtained from other methods, none of these barrier heights is less than that for the bare junctions. We suggest that the presence of GaAs-oxide at the periphery of the (Pd/dC−X/GaAs) molecular domains can explain these results.[97] The *C*−*V*-derived SBH values are averaged over all of the Pd/dC−X/GaAs domains, i.e., including the presumed Pd/dC−X/oxide/GaAs sites at the periphery. With such an oxide layer below the molecular domains, all the barrier heights for Pd/dC−X/GaAs domains can be higher than that of the bare surface. Our suggestion is supported by the observation that the *C*−*V*-derived barrier for bare Au/n^--GaAs junctions, which we have assumed to have GaAs-oxide at their interface, is between the values for junctions modified with negative and positive molecular dipoles (see Supporting Information, Table 2S). Because in most cases transport through the Pd/dC−X/oxide/GaAs sites will be negligible compared to that via the surrounding Pd-dC−X-GaAs and pinhole sites, *I*−*V* will not be sensitive to the barriers under those domains, whereas the IPE measurements will be weighted in favor of the regions without oxide and molecules.

5.3 Pd vs Au, in Terms of Molecular Effects on Junction Characteristics. Importance of the Microscopic Nature of Interface. The striking result of Figs 6, 8a and, to a lesser extent, Figs 5b and 9 is the inversion of the molecular effect, depending on the evaporated metal.

Experimentally, we observe drastic morphological differences between the metal pads, depending on whether they grow in a 3D or 2D manner. Whereas Pd grows in a 2D manner, Au growth is typically 3D because of its poor wetting properties (cf. Supporting Information, section 6).[42,98] Such 3D growth normally yields larger-size clusters than the 2D growth of Pd.[98,99] For Au, the 3D growth leads to an interface with Au mostly overgrowing the molecules, whereas for Pd, the 2D growth leads to intimate contact between metal and molecules. These differences in the metal/monolayer interface can explain the apparent difference in charge distribution at the interface.

Evidence for the net (relative) dipole direction comes from the experimentally determined direction of the change in barrier height by assuming that this direction depends on the dipole of the molecules, making up the layer (electron-withdrawing or electron-donating). For Au, the direction of change fits with the dipole direction of the free molecule and that found for the molecular film on a free surface. For Pd, the change in barrier height is opposite to that expected from the dipole direction of free molecules. Therefore, in the case of Au, the poles of the dipole remain as in the free molecule, whereas for that of Pd, the interaction between molecule and spill-over electron density outside the metal surface inverts the free molecule dipole, as explained earlier.[36,42] The smaller molecular effect that is deduced from the IPE and *C*−*V* data for junctions with Pd than with Au may be due to some overgrowth of Pd over the molecular domains, i.e., regions where there will not be dipole inversion. The effect of such regions will be least pronounced in the *I*−*V* data, for reasons explained above.

5.4 Assessing Effective/Nominal Contact Area Ratios. Regardless of the measurement technique used, the finding that the *C*−*V*-derived ratio S_{eff}/S_{geom} (Table 4) and nearly all the corresponding values, derived from the *I*−*V*−*T* data (f_1, f_2; cf. Table 3), for evaporated contacts are >1 can be ascribed to the roughness of the GaAs surfaces (0.5−1 nm), to metal penetration into the GaAs substrate (as is the case with Au),[82−84] and to metal penetration beneath the molecular domains (especially when Au is used).[42,90,100,101] Consistent with these arguments, all the values of f_i (i = 1, 2; the ratio between effective and geometrical surface areas at zero bias, derived from *I*−*V* measurements; cf. eq 7), on LOFO-made junctions are <1 (cf. Table 3). The reason is that LOFO-made contacts, which are "ready-made" ones, are unlikely to penetrate into small pinholes. The probability of metal penetration increases with increasing pinhole size (as indicated by $f_1 > f_2$; cf. Table 3). Naturally, the surface of a LOFO-made pad that will contact the molecularly modified surface can only be as smooth as the glass on which the pads were deposited (0.5−1 nm) but is likely to be rougher because the lift-off process includes etching the glass/metal pad interface.[38,55] The resulting degree of roughness, together with the ∼1 nm thickness of the *discontinuous* molecular film of dC−X, will allow for some direct contact between the LOFO-made pad and the GaAs.

For bare samples, the *C*−*V*-derived S_{eff}/S_{geom} ratio is higher for the bare Pd/n^--GaAs (= 1.95) than for the Au/n^--GaAs (= 1.57) junction, as shown in Table 4. This result can be explained by the 2D growth of Pd, which tends to provide better surface coverage than the 3D growth of Au.[42,98,99] The same explanation holds for the difference between the molecularly modified samples, contacted by indirectly evaporated Pd and Au (e.g., Pd/dC−X/n^--GaAs vs Au/dC−X/n^--GaAs).

The lower S_{eff}/S_{geom} ratios found for the Pd/dC−X/n^--GaAs and Au/dC−X/n^--GaAs junctions than those for the bare Pd/n^--GaAs and Au/n^--GaAs ones can be ascribed to the preferred Au deposition and growth in the pinholes. For Au, this induces 3D growth in the vicinity and far away from the pinholes (cf. ref 42 for more details), so that the Au can overgrow most of the molecular domains. For Pd, it is likely that 3D growth happens in the pinholes,[102] whereas 2D growth occurs on the molecular domains. In each case, the contribution of the 3D growth leads to lower effective contact areas between the metal and the semiconductor and, accordingly, to lower a S_{eff}/S_{geom} ratio than is the case without the molecules.

The higher f_2 values, derived from the *I*−*V* data, for the Au/dC−CH_3/n^--GaAs and Au/dC−CF_3/n^--GaAs junctions than for the Pd/dC−CH_3/n^--GaAs and Pd/dC−CF_3/n^--GaAs ones can be attributed to the much enhanced probability of Au penetration into point and line defects in the molecular layer[90,91] (apart from filling the small and large pinholes), compared to Pd.[36]

5.5 Differences between High- and Low-Doped *n*-GaAs. We now discuss how changing the doping concentration can so drastically change the electrical properties of junctions that are modified with the same set of dicarboxylic derivatives. It is this comparison that allows us to draw the major conclusion

(97) Before contacting the molecularly modified surfaces, there will be some oxide in the pinholes and (at least) under the outer regions of dC−X/GaAs domains (because it should be relatively easy for O to reach there). After contacting, Pd but not Au reacts with and removes the GaAs−oxide in the pinhole areas only, leaving behind oxides below the molecularly modified domains.

(98) Li, Y.; DePristo *Surf. Sci.* **1996**, *351*, 189−199.
(99) Schmidt, A. A.; Eggers, H.; Herwig, K.; Anton, R. *Surface Science* **1996**, *349*, 301−16.
(100) Ohgi, T.; Sheng, H.-Y.; Dong, Z.-C.; Nejoh, H. *Surf. Sci.* **1999**, *422*, 277−282.
(101) Wang, B.; Xiao, X.; Sheng, P. *J. Vac. Sci. Technol., B* **2000**, *18*, 2351−2358.

(102) This can happen due to deposition of Pd clusters directly on the pinholes and/or diffusion of clusters from the molecular domains into the Pd-filled pinholes.

from this work, viz. *molecules that form incomplete, nonideal monolayers can control semiconductor−metal junctions*. As this is clear already from the raw electrical measurements of junctions with n^+-GaAs,[51] the question arises why we need the analyses that we have presented here to find similar molecular effects with n^--GaAs (cf. Figure 6)?

To answer this, we note that our analysis of the n^+-GaAs experimental results assumed homogeneous electronic charge transport through the junction.[37,39,51] Using this simple model, we found that one SBH describes transport through the n^+-GaAs junctions. This result implies that in these samples there is only one effective SBH, even if coverage is less than a monolayer. One possibility is that most pinholes are smaller than the surrounding molecular domains and, thus, are affected/controlled by the adjacent molecules (cf. Supporting Information, section 3; case of pinholes smaller than the surrounding molecular domains, $d_1 < d_2$). Estimates, based on the molecular coverage of n^+-GaAs, deduced from the FTIR data (cf. Table 1) and from TOF SIMS experiments,[32,36,42] assuming a homogeneous distribution of pinholes, show that the size of pinholes in these samples is at least 5 times less than that of the surrounding molecular domains, consistent with our explanation. This picture suggests that the molecular dipole domains on the n^+-GaAs samples affect the entire junction in a relatively uniform fashion because of the molecules' effect on the semiconductor region near the interface (cf. Figure 4b). In such a case, the SBHs in the molecular domains and the pinholes will be similar, which makes the entire interface electrically homogeneous for $C-V$ measurements. Because tunneling through metal−dC−X-GaAs contacts is less favorable than transport through the pinholes, the $I-V$ results of the n^+-GaAs samples reflect only transport through the latter. Therefore, the $I-V$ characteristics on these samples fit those for *homogeneous electrical transport*, as approximated (using the concept of an effective barrier height) by the thermionic emission model.[37,39]

In n^--GaAs samples, the coverage of dC−X molecules is 1.3−1.5 times less than that on n^+-GaAs, as shown by comparing FTIR, contact angle, and XPS data for the dC−CF_3-covered surfaces (cf. Table 1), which, on the basis of the XPS data, is somewhat below and above 50% for low and high-doped GaAs, respectively. The finding that we cannot use a homogeneous barrier model to analyze the IPE, $C-V$, and $I-V$ data for the n^--GaAs junctions but can use an inhomogeneous barrier model suggests that there is more than one effective SBH, even though this is not obvious from the raw $I-V$ data. The reason for this will be explained next.

The results of the model with a double-Gaussian distribution of barriers (eq 7), used to analyze the $I-V-T$ data, indicate that the monolayer on n^--GaAs is such that there are two types of pinholes, those that are pinched-off and (larger) ones that are not pinched-off. These pinholes have dimensions smaller and larger than the local molecular domains surrounding them (and than the depletion layer of the semiconductor below them), respectively.

In the $I-V$ measurements, the (apparent) SBH of an inhomogeneous Schottky barrier reflects the different SBHs according to their relative contact areas. The 1.5−2.2 higher effective area of the larger pinholes than that of small ones thus suggests that the $I-V$ measurements are controlled by the previous one. Also, in IPE, most of the photocurrent will be collected through the large pinholes.

In $C-V$, the region with the higher effective area (i.e., geometric area, corrected for relative charge density in the semiconductor) controls the measured electrical properties. This suggests that the raw $C-V$ measurements of the metal/dC−X/n^--GaAs junctions show the characteristics of pinholes, which have an effective area larger than that of the molecular domains (cf. Tables 3 and 4 and section 5.4).

Thus, we see that with all the techniques, the measurements will be dominated by the large pinholes that are not affected by the molecules. This explains why the simpler data analysis, used for n^+-GaAs-based junctions, does not show any clear molecular effects.

Why does adsorption of dC−X on n-GaAs yield higher coverage on high- than on low-doped samples? In a recent study, it was found that 1-octadecene monolayers systematically give less ordered films on H-terminated n^+-Si(111) surfaces than on n^--Si ones.[103] This finding was explained by realizing that the n^+-Si surface Fermi level lies very close to the conduction band ($E_c - E_f < 0.17$ eV). Therefore, almost all of the Si dangling bonds will be saturated with two electrons. This situation will impede the reaction of 1-octadecene, which requires an unsaturated (neutral) dangling bond on the Si. The direct result is that formation of a Si−C bond by addition of 1-octadecene on n^+-Si is more difficult than on n^--Si ($E_c - E_f = 0.30$ eV; dangling bonds are mainly occupied by a single electron or neutral).[103]

With this introduction and adopting Wolkenstein's theory for chemisorption[104,105] for the dC−X molecules on our GaAs surfaces, we argue that chemisorbing dC−X molecules contributes to the semiconductor's surface charge, which must be balanced by a space charge in the adjacent region, to maintain electro-neutrality. The dC−X binding groups will be present in solution both as charged (COO^-) and as neutral (COOH) species, due to the presence of small amounts of water,[71,106] similar to what is known for a number of other systems.[17,107−109] We know that chemisorption of carboxylic acids on ambient exposed GaAs leads to a bridging mode chemical bond.[53] During chemisorption of dC−X on n-GaAs, the COOH binding group captures an electron from the semiconductor and adsorbs on the surface according to an electrochemical half reaction like the following:

$$2(-Ga-OH_{surface}) + HO_2C-R + e^- \rightarrow -Ga_2-O_2C-R_{surface} + H_2O + OH^-$$

(103) Miramond, C.; Vuillaume, D. *J. Appl. Phys.* **2004**, *96*, 1528−1536.
(104) Wolkenstein, T. *Electronic Processes on Semiconductor Surfaces During Chemisorption*; Consultants Bureau: New York, 1991.
(105) Rothschild, A.; Komem, Y.; Ashkenasy, N. *J. App. Phys.* **2002**, *92*, 7090−7097.
(106) This is consistent with our earlier observation that dC−OCH_3 requires intentional addition of small amounts (4% v/v) of water to accomplish the adsorption properly (cf. refs 38 and 39). This need was ascribed to the high concentration of negative charge on the binding group that results from the negative dipole. This negative charge favors the formation of the radical or the carboxylate form, compared to what is the case for molecules with a positive dipole. Adding water screens the charge and decreases the activation energy barrier, thus allowing their (slow) adsorption.
(107) Schwartz, D. K. *Annu. Rev. Phys. Chem.* **2001**, *52*, 107−137.
(108) Love, J. C.; Estroff, L. A.; Kriebel, J. K.; Nuzzo, R. G.; Whitesides, G. M. *Chem. Rev.* **2005**, *105*, 1103−1169.
(109) Schreiber, F. *Prog. Surf. Sci.* **2000**, *65*, 151−256.

where R stands for the remainder of the dC−X molecule. The cycle can be completed by the OH^- reacting on the surface (e.g., $GaAs_{surface} + OH^- \rightarrow GaAs{-}OH_{surface} + e^-$). Therefore, the higher the donor density in the *n*-GaAs, the more free electrons are available in the conduction band for this process, and dC−X coverage increases with increased semiconductor doping.[105,110] Chemisorption of a $R{-}COO^-$ species on the *n*-GaAs surface is less likely due to repulsion (i.e., higher activation energy) with the negatively charged surface. For *p*-GaAs surfaces, results for which were presented elsewhere,[39] chemisorption will likely be via $R{-}COO^-$ on the positively charged *p*-GaAs surface.

6. Conclusions

Our results show how molecules that do not form well-organized continuous films can control one of the most ubiquitous of all electronic device components, the metal/semiconductor junction. The only condition to be fulfilled is that, on the average, the adsorbed molecules will have a dipole moment perpendicular to the surface. The first major implication of this work is that one can consider many more types of molecules for incorporation in active electronic devices than what was considered hitherto. The reason that relatively poorly organized, incomplete, molecular monolayers can be considered is because a layer of dipoles affects the interface beyond the lateral dimensions of the molecular domain, i.e., into the semiconductor, reaching also below the adjacent pinhole areas, located *between* adjacent molecular pinholes. This molecular effect depends to a large extent on the difference in barrier height for electron transport between adjacent domains, the molecular coverage on the surface, the concentration and size of both large pinholes and small pinholes, and the doping level of the semiconductor. Metal/monolayer/semiconductor interfaces that contain pinholes that are smaller than the surrounding molecular domains (irrespective of whether they are homogeneous or inhomogeneous) show homogeneous electrical properties. Our results suggest that even half coverage may suffice for this. Interfaces that are similar but that have also pinholes that are larger than the surrounding molecular domains show inhomogeneous electrical properties. In principle, this may occur even at high coverage, but it clearly becomes more likely the lower the coverage. In this case, theoretical models that take into account the inhomogeneous electrical effects, via, for example, parallel conduction model, are required to interpret the electrical characterization data. Indeed, although *I*−*V*, *I*−*V*−*T*, *C*−*V* and IPE measurements all can serve as a useful tool to estimate the electrostatic effects of homogeneous molecular layers, they should be interpreted carefully if the layer is inhomogeneous. An important corollary to these conclusions is that it becomes actually desirable that molecules at the metal/semiconductor interface do not form continuous films because:

(1) molecule stability during electron transport will be much less (or even a non-) issue as it is possible that most of the current will flow between the molecules, rather than across them;

(2) a continuous molecular layer will generally form a transport barrier. Unless the molecules form a very narrow film (say, <5 Å) or are electrically conducting (e.g., highly aromatic or otherwise conjugated), such a barrier will be especially detrimental for the use molecular monolayers at organic semiconductor/electrode interfaces, to control injection across such interfaces by tuning the electrode work function.[111]

Finally, the comparison between high- and low-doped GaAs teaches that, even if no clear molecular effects are found initially, changing semiconductor doping can be one way to reach coverage sufficient for the molecular field effect.[47]

Acknowledgment. D.C. and H.H. thank the Israel Science Foundation, the Philip M. Klutznick Research Fund, the G.M.J. Minerva Centre for Supramolecular Chemistry, and the Minerva foundation (Munich) for partial support. We thank our Weizmann Institute colleagues Olivia Niitsoo and Jamal Ghabboun for experimental assistance, R. Arad-Yellin and A. Shanzer for the dC-X molecules, and H. Cohen for XPS measurements. We thank A. Kahn (Princeton University) and A. Vilan (Weizmann Institute of Science) for fruitful discussions, G. Bruno (CNR-IMIP, Bari), V. Augelli, L. Schiavulli, and D. Loiacono (University of Bari) for their support, J. Pelz, C. Tivarus (Ohio State University), and the reviewers for critical and constructive comments on the manuscript. D.C. holds the Schaefer chair in Energy research.

Supporting Information Available: 1. Basic assumptions inherent in the (photo) electrical measurement techniques for semiconductor/metal junction characterization. 2. Classic models in (photo) electrical measurement techniques. 3. Theoretical considerations. 4. Effect of molecular domains on the (photo)-electrical measurements. 5. Comparison between SBHs of different bare metal/*n*-GaAs junctions. 6. Wetting properties of Au and Pd. This material is available free of charge via the Internet at http://pubs.acs.org.

JA058224A

(110) For our samples, assuming all other factors being equal, the higher dopant concentration in high-doped *n*-GaAs was found to give a ~10 times higher net (negative) surface charge than the low-doped *n*-GaAs, both before and after dC−X adsorption.

(111) To increase injection efficiency with the help of an interfacial layer of molecules (excluding "conducting" ones, for which different conditions apply), the layer should be porous with maximal length of edges/area, to give highly a strongly inhomogeneous lateral electric field distribution and with a polarity to lower the barrier.